

REVIEW

Organometallic Langmuir-Blodgett films for electronics and photonics

Hari Singh Nalwa* and Atsushi Kakuta

Hitachi Research Laboratory, Hitachi Ltd, 7-1-1 Ohmika-cho, Hitachi City, Ibaraki 319-12, Japan

This review provides a brief introduction to the Langmuir-Blodgett (LB) technique and to the utilization of ultrathin films in the fields of electronics and optics. The electrical and nonlinear optical properties of the Langmuir-Blodgett monolayer and multilayers of organoruthenium complexes, ferrocene derivatives, metal(4,5-dimercapto-1,3-dithiol-2-dithiolene)₂ complexes, metallophthalocyanines, metalloporphyrins, metal(dibenzotetra-aza[14]annulene)s and siloxane polymers are presented. Possible applications of organometallic LB films in sensors, electroluminescence and electrochromic devices, optical switches, solar cells, infrared detectors and harmonic generators are discussed.

Keywords: Langmuir-Blodgett technique, ultrathin films, organometallic compounds, electrical properties, nonlinear optical properties, electronics, photonics, buckminsterfullerene

CONTENTS

- 1 Introduction
- 2 Langmuir-Blodgett (LB) technique
 - 2.1 Molecular considerations
 - 2.2 Preparation of LB films
- 3 Organometallic LB films for electronics
 - 3.1 Pyroelectric LB films
 - 3.2 Electrically conducting LB films
- 4 Organometallic LB films for nonlinear optics
 - 4.1 Second-order nonlinear effects in organometallic LB films
 - 4.2 Third-order nonlinear effects in organometallic LB films
- 5 Possible applications
- 6 Conclusions
- References

1 INTRODUCTION

Organic materials that exhibit useful electrical, optical, magnetic, thermal and mechanical properties have been considered as the key elements for future technological development. Organic materials provide tremendous opportunities to amend chemical structures in accordance with particular requirements. By knowing the basic fundamental units that generate a particular effect of interest, organic molecules can be designed, synthesized and applied to novel devices. Specialty materials are required in order to achieve desired properties. For example, only noncentrosymmetric polar materials can display piezoelectric responses and optical second harmonic generation. A material with a long π -conjugated system is a good candidate for achieving higher electrical conductivity and third-order optical nonlinearity. On the basis of electrical properties, materials can be divided into two main groups:

- (1) dielectrics which are highly insulating materials, and
- (2) semiconductors or metals which possess high electrical conductivity.

Polar dielectrics form an important class of electronic materials since they exhibit piezoelectric, pyroelectric and ferroelectric properties. Organic π -conjugated materials show interesting semiconducting and metallic properties; hence they have been considered potential candidates as a replacement to inorganic semiconducting or metallic materials. Both polar dielectrics and π -conjugated materials could be used in the field of nonlinear optics.

The selection of materials for a specific end use is an important task. In fact, to design a specialty material, the precise approach involves several steps: design and molecular modeling, chemical syntheses, material processing, spectroscopic analysis, evaluation of physico-chemical proper-

* To whom correspondence should be addressed.

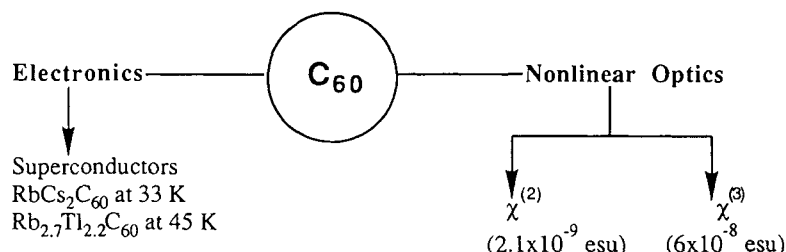


Figure 1

ties to establish a structure–property relationship, molecular engineering to optimize desired functions, and fabrication into devices.

A variety of organics and organometallics will be discussed in this article. To show the importance of the novel materials, we take here an example of the C_{60} species. C_{60} (Buckminsterfullerene) forms a variety of organometallic compounds and can be prepared in ultrathin films by vacuum evaporation and as Langmuir–Blodgett films at the air–water interface. Interestingly, C_{60} also shows both unique electrical and nonlinear optical properties, which coincides with the review presented here. Therefore, in the course of this article, a brief introduction to C_{60} is provided.

The C_{60} buckminsterfullerene is a new form of carbon that has a soccer-ball structure and is a higher carbon cluster.^{1,2} Highly stable C_{60} is an icosahedral-cage molecule. The solid C_{60} species is a polygon with 60 vertices and 32 faces, 20 of which are hexagonal and 12 pentagonal. It is an aromatic molecule where all valences are satisfied at the outer and inner surfaces, which give rise to an ocean of π -electrons. The diameter of the C_{60} molecule is approx. 0.7 nm and it is capable of incorporating a variety of atoms.³ An area of *ca* 1 nm² has been calculated from the cell parameters of the crystals of C_{60} .⁴

Langmuir–Blodgett films of C_{60} with and without matrix molecules have been developed.^{5,6} At room temperature the C_{60} molecules are orientationally disordered, whilst below 249 K the molecules become orientationally ordered and correspond to a symmetry change from Fm3 to Pa3.⁷

Doped C_{60} polycrystalline powders show sharp superconducting transitions at 19 K in K_3C_{60} ,⁸ at 33 K in Cs_2RbC_{60} ,⁹ and at 45 K in $Rb_{2.7}Tl_{2.2}C_{60}$.¹⁰

Interestingly, C_{60} also exhibits both second-order and third-order nonlinear optical effects. C_{60} has a third-order nonlinear optical susceptibility ($\chi^{(3)}$) of 6×10^{-8} esu in benzene solution at 1064 nm as estimated by using a degenerate four-wave mixing technique.¹¹ A $\chi^{(3)}(-3\omega; \omega, \omega, \omega)$ of

2×10^{-10} esu for C_{60} thin films at the same fundamental wavelengths from third-harmonic generation measurements has been determined.¹² In addition, a bulk second-order nonlinear susceptibility $\chi^{(2)}$ of 2.1×10^{-9} esu for C_{60} thin films using 1064 nm pulses from a Nd:YAG laser was recently reported.¹³ The $\chi^{(2)}$ is 10 times larger at 140 °C than its value at room temperature.

C_{60} can be derivatized to break its spherical symmetry. C_{60} reacts with electron-rich reagents and its double-bond reactivity is close to that of very electron-poor arenes and alkenes. Laser vaporization of a variety of carbonaceous materials such as polyimides, coal and polycyclic aromatic hydrocarbons yields C_{60} . Higher fullerenes such as C_{76} , C_{84} , C_{90} , C_{94} and $C_{70}O$ can be isolated and spectroscopically characterized.¹⁴ Even-numbered carbon clusters with giant structures having as many as 600 carbon atoms can be formed by laser deposition of soot.¹⁵

C_{60} is one of the most extensively investigated organic materials in the last few years.¹⁶ It not only shows conductivity and semiconductivity¹⁷ but also forms a variety of metal complexes.¹⁸ Studies of its physical properties demonstrate the superiority of compositions of C_{60} over other organic and inorganic materials due to their excellent thermal and environmental stabilities, ease of chemical modification, good adhesive properties and ease of fabrication into ultrathin films. Ultrathin films of C_{60} and its organometallic complexes offer unique chemistry and physics which can be applied to future technologies in the fields of electronics and photonics and to many other fields of science (Fig. 1).

Material processing is one of the most important factors in fabricating devices. Organic materials can be processed into single crystals, sheets, thin films, and liquid crystals. For solid-state applications, thin films of desired organic materials are fabricated with the aid of processing techniques such as sputtering (ion beam, magnetron or electrical sputtering), chemical vapor deposition, vacuum evaporation (thermal evapora-

ation, ionized cluster beam or molecular beam epitaxy), spin-coating and casting. In the case of electroactive polymers, thin films are obtained by electrochemical polymerization on a metal electrode. In these techniques, precise control of the film thickness is not feasible and molecules are randomly oriented, though molecular orientation in free-standing films can be introduced by mechanically stretching the films to several times of their original length followed by an electrical poling-freezing process.¹⁹ It is likely that a preferential orientation can also be achieved in spin-coated films by employing the same poling technique, though the degree of molecular orientation attained by the electrical poling process may not be sufficiently high.

The increasing importance of ultrathin films in electronic technologies has recently intensified research in the design and synthesis of organic materials where film thickness can be precisely controlled, and a high degree of preferential molecular orientation can be achieved as well. The usefulness of highly ordered microstructures has been realized in the fields of molecular electronics, nonlinear optics and bioengineering. The Langmuir-Blodgett (LB) technique is one of the most powerful tools that offers an avenue to align and control individual microstructures at the molecular level.

By the LB technique, closely packed, uniformly oriented and controlled-thickness monolayers and multilayers of desired amphiphiles can be deposited onto a solid substrate. As a result, the applicability of the LB technique could be broad, in multidisciplinary fields of science. With this view, a very wide variety of organic molecules have been tailored for specific purposes to prepare organized molecular assemblies at interfaces. It is equally important to utilize organometallic structures for these purposes since they also offer unlimited architectural flexibility to establish structure-property relationships.

An apparent feature that distinguishes organometallic from organic systems is charge-transfer transitions due to metal-ligand bonding. In organometallics, the diversity of metals, oxidation states and ligands plays a major role in optimizing charge-transfer interactions. The overlapping of the π -electron orbitals of conjugated ligands with the metal-ion d-orbitals gives rise to large intramolecular interactions. From nonlinear optics aspects, a large difference in the electronegativities of metal and carbon atoms assists in generating large polarities in organometallic com-

pounds. Langmuir-Blodgett films have been considered the key elements for future molecular technologies for fabricating devices at molecular level. The LB technique, which provides processing up to a molecular level, assists in building up desired microstructures that display all these electronic and photonic functions. The controlled film thickness and molecular ordering yielded by the LB technique are the main factors that suggest its applicability not only in microelectronics but also in other fields of science. This aspect has been reflected by rapid growth of the research activities in LB films.

No full description of organometallic LB films is currently available. The present review therefore is a first attempt to summarize results on electrical and nonlinear optical properties of organometallic LB films. To introduce readers to this field, a brief introduction to the LB technique, amphiphiles and microstructures of monolayer and multilayers is provided. In particular, the importance of the LB technique in the field of molecular electronics and optoelectronics is discussed.

2 LANGMUIR-BLODGETT (LB) TECHNIQUE

The formation of monolayers at a water surface has been known for centuries. In the 18th century, Franklin²⁰ first documented the formation of a layer of oil on a water surface by spreading oil droplets on water. After almost a century, Pockels²¹ demonstrated the preparation of the first monolayer at the water-air interface by pushing a soap film at a water surface. In 1899, Rayleigh²² described the nature of the monolayers and evaluated the size of a surfactant molecule. In 1917, Langmuir²³ published the first systematic study of monolayers of amphiphilic molecules at the water-air interface. In 1935, Katharine Blodgett²⁴ carried out the first detailed study on the deposition of multilayers of long-chain carboxylic acids onto a solid substrate. Langmuir and Blodgett²⁵ together investigated the details of deposition conditions and the structure of long-chain fatty acid multilayers by depositing multilayers onto a glass substrate. In 1932, Irvin Langmuir was awarded the Nobel Prize in Chemistry for his pioneering work in the field of surface science. Historical developments in the

field of Langmuir–Blodgett films have been compiled by Gaines.²⁶

The importance of LB films can be realized from the fact that the First International Conference on Langmuir–Blodgett films was organized in 1982 at Durham, UK, the Second in 1985 at Schenectady, USA, and thereafter conferences have continued to be held in alternate years. They cover all aspects of LB films, and presentations are published in the periodical, *Thin Solid Films*. Though research on LB films is published in a variety of periodicals, a few years ago the American Chemical Society launched the *Langmuir* periodical, covering studies on various aspects of LB films. The LB technique has been widely used in biology for fabricating monolayers and multilayers of lipids and proteins. The LB films of enzymes and antibodies have been used as biosensors, using enzyme-immobilized lipid monolayers. Recently, organic LB films have been attracting attention in the fields of electronics and nonlinear optics.

2.1 Molecular considerations

An amphiphile is an organic molecule consisting of a hydrophilic end (preferentially a water-soluble part) and a hydrophobic end (a water-insoluble part). The hydrophilic end of an amphiphile sticks to the water subphase while the hydrophobic end resides above the subphase. Structures of some amphiphilic molecules are shown in Fig. 2 and hexadecanoic (palmitic) acid $[\text{CH}_3(\text{CH}_2)_{14}\text{COOH}]$, octadecanoic (stearic) acid $[\text{CH}_3(\text{CH}_2)_{16}\text{COOH}]$, icosanoic (arachidic) acid $[\text{CH}_3(\text{CH}_2)_{18}\text{COOH}]$, ω -tricosenoic acid $[\text{CH}_2=\text{CH}(\text{CH}_2)_{20}\text{COOH}]$, docosanoic (behenic) acid $[\text{CH}_3(\text{CH}_2)_{20}\text{COOH}]$ are well-known examples of amphiphiles. These fatty acids (e.g. $\text{C}_n\text{H}_{2n+1}\text{COOH}$, where generally $n > 12$), possessing long hydrocarbon chains with a highly polar COOH end, are the most suitable materials for developing LB films. In these acids, the long hydrocarbon chain is the hydrophobic part, while the carboxylic group is the hydrophilic part. This structural amphiphilicity is a prerequisite for an LB molecule, though non-amphiphilic molecules can be deposited by using an appropriate solvent and mixing with fatty acids.

The structural amphiphilicity has to be considered when designing LB molecules for specific purposes. Figure 2 shows the general structure of the amphiphiles. A special unit such as a conjugated system may be incorporated as part of the

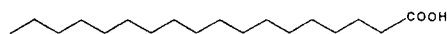
amphiphile. In addition, either of these parts may be utilized as a functional group. Amphiphiles of dyes and polymers can be developed. This review focuses on the electrical and nonlinear optical properties; therefore the details of specialty LB molecules suitable to their function will be discussed in the following sections.

2.2 Preparation of LB films

The deposition of molecular monolayers by the LB technique is not a straightforward process, but involves several preliminary steps before a monolayer is obtained. The deposition process is carried out in a dust-free clean room. The fabrication of the monolayer is affected by the concentration of solute, temperature, surface pressure, barrier speed, subphase and the subphase pH. Mostly, the subphase is water or aqueous solutions but mercury, glycerol and other liquid subphases can be used. The monolayer is transferred to a clean solid substrate such as glass slides, quartz plate, metal-coated slides, mica and silicon wafers. Organic solvents used for spreading the monolayer are generally water-insoluble, such as chloroform, hexane, benzene, toluene and xylene. Sometimes acetone and alcohols are added to those solutions depending upon the solubility of the amphiphiles. In a typical deposition procedure, three steps are performed;

- (1) *Spreading* a monolayer of an amphiphilic molecule in a volatile solvent leaves a monolayer of the amphiphile on the subphase.

Stearic acid



Arachidic acid



ω -Tricosenoic acid

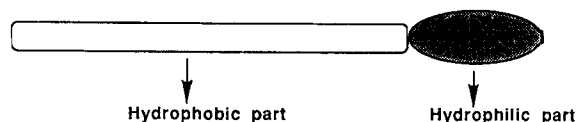
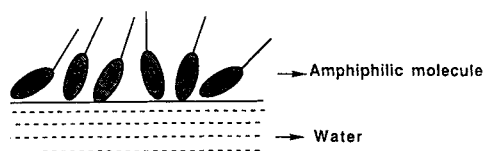
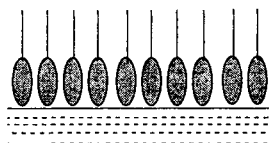


Figure 2 Structure of an amphiphile having a hydrophilic end and a hydrophobic end.

(1) Spreading

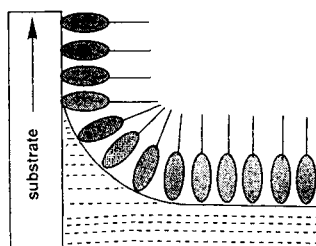


(2) Compression

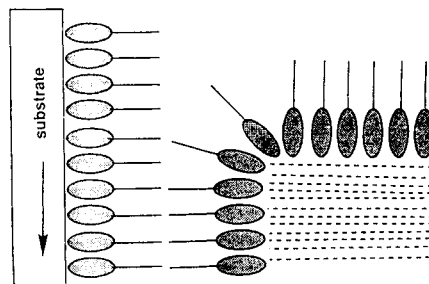


(3) Deposition

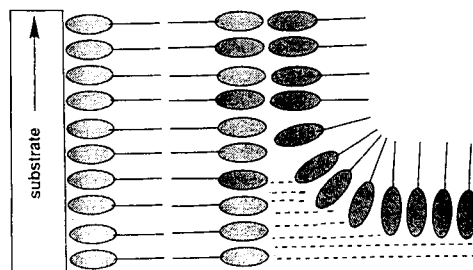
(First Layer)



(Second Layer)



(Third Layer)

**Figure 3** Deposition of a monolayer from the air–water interface.

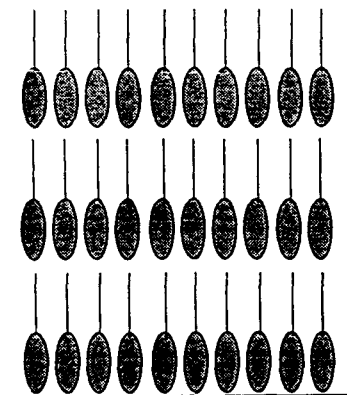
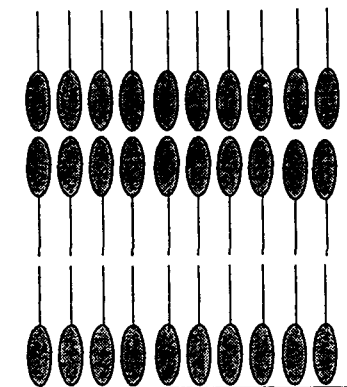
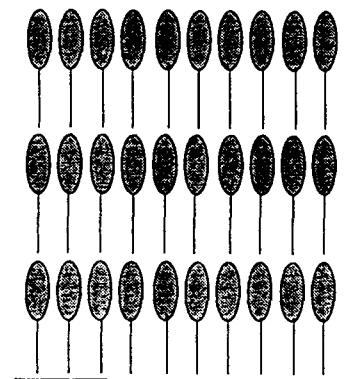
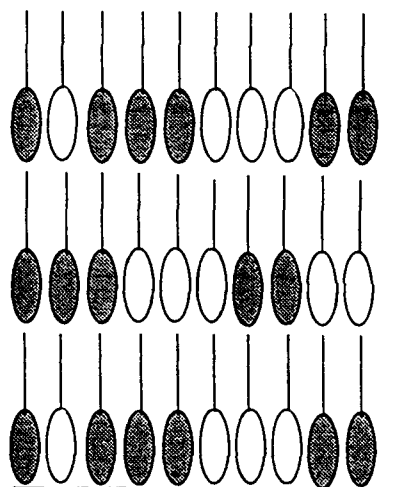
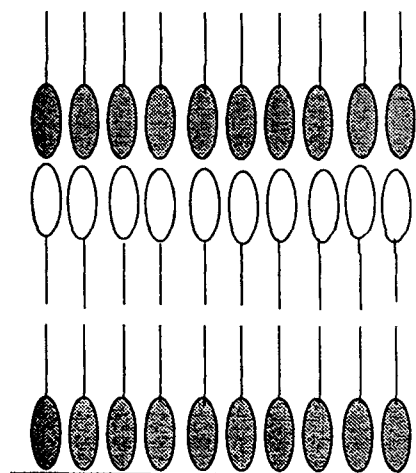
X-type LB film**Y-type LB film****Z-type LB film****Mixed LB films****Alternate LB films**

Figure 4 X-, Y-, and Z-type modes of monolayer stacking and heterotype LB films in a mixed and in an alternating layer. (Shaded amphiphile is functionalized, non-shaded is a fatty acid amphiphile.)

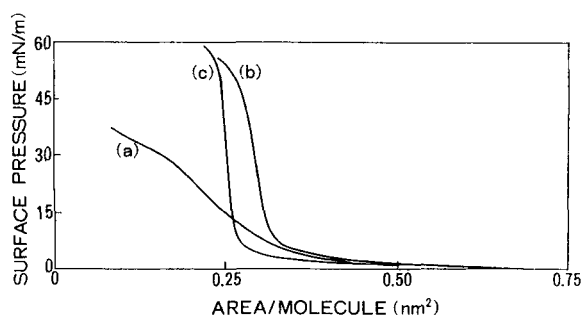


Figure 5 Surface pressure-area isotherm of *N,N'*-dioctadecyl-2,4-dinitro-1,5-diaminobenzene (DIODD): (a) pure DIODD; (b) 1:1 mixture of DIODD; arachidic acid; (c) 1:3 mixture of DIODD and arachidic acid. (After Ref. 27.)

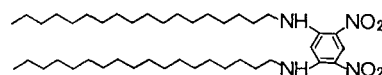
- (2) *Compression* is started after incubation for several minutes. By moving a barrier, the surface pressure increases and the molecules are closely packed and uniformly aligned.
- (3) *Transfer* of a monolayer from aqueous subphase onto a solid substrate is carried out at a particular deposition rate and at a defined surface pressure, depending upon the nature of the amphiphilic molecule.

Figure 3 shows the details of monolayer formation and molecular orientations. Not all amphiphiles yield stable monolayers and crystals may be formed. This instability hinders transfer of the monolayers onto solid substrates. In such cases, a fatty acid is mixed with the amphiphile to improve the monolayer stability. The long-chain fatty acids such as stearic acid, arachidic acid, behenic acid and ω -tricosenoic acid work as a transfer promoter. Generally, monolayers are deposited with long-hydrocarbon-chain acids since it gives rise to stability. The stability of monolayers can be improved by molecular engineering of amphiphiles by amending their chemical structures.

Figure 4 shows the modes of monolayer stacking. LB monolayers on a substrate stack in three different ways, depending upon the nature of the LB molecule. The tail-to-head and tail-to-head configurations, as seen from a substrate, are called X-type stacking. The head-to-tail and head-to-tail modes of stacking are referred to as Z-type LB films. The head is a hydrophilic end and the tail is a hydrophobic end. The most common head-to-head and tail-to-tail mode of stacking is referred to as Y-type LB film. In a Y-type LB film, alternating monolayers are deposited with long-chain acids. The alternating layers deposited in the Y-mode may lead to noncentro-

symmetric structures required for second-harmonic generation.

Figure 5 shows a schematic isotherm of a nonlinear optically active two-dimensional charge-transfer amphiphile, *N,N'*-dioctadecyl-2,4-dinitro-1,5-diaminobenzene (DIODD; compound I) on a water subphase.²⁷ The π -*A* isotherm describes the variation of surface pressure versus surface area per molecule of pure DIODD molecules and DIODD chromophores mixed with arachidic acid in 1:1 and 1:3 molar ratios, respectively. We can determine the area per molecule. A surface area of 0.49 nm² per molecule was calculated for the DIODD molecule and the surface area of a 1:1 mixture is approx. 0.30 nm² per molecule on average. Arachidic acid was used as a transfer promoter for DIODD. Therefore, a π -*A* isotherm provides information on the stability of the LB monolayers at the water-air interface, molecular orientation and phase transitions.



I *N,N'*-dioctadecyl-2,4-dinitro-1,5-diaminobenzene (DIODD)

The transfer of a monolayer from the water-air interface onto a solid substrate can be accomplished in two ways: (1) vertical dipping, and (2) horizontal lifting.

The importance of LB films has been accepted in the fields of electronics and optics because they offer the following advantages:

- (1) a high degree of molecular orientation;
- (2) precise control of film thickness at a molecular level;
- (3) control of layer architecture;
- (4) building up of noncentrosymmetric structures for nonlinear optics.

3 ORGANOMETALLIC LB FILMS FOR ELECTRONICS

In this section, the LB molecules that have been assessed as to their potential for the field of electronics are discussed. Electronic functions such as dielectric constant, dielectric loss and dielectric breakdown strength, and electret properties such as pyroelectricity, piezoelectricity and ferroelectricity, have been well investigated for organic

molecular and polymeric dielectric materials. Conductivity properties have been studied in π -conjugated materials. Organometallic materials have various electronic properties that are similar to those of organic materials. Because not all these properties have been studied in organometallic LB compounds we will mainly emphasize here the pyroelectric properties of organometallic LB films which have been reported by a group at Oxford, and also electrically conducting organometallic LB films will be discussed.

3.1 Pyroelectric organometallic LB films

For the general reader, a brief description is now given of electrical properties such as pyroelectricity, piezoelectricity and ferroelectricity which are closely related to the crystalline structures of the materials.

Crystalline materials can be classified into 32 crystal point-group symmetries, out of which 11 are centrosymmetric and 21 are noncentrosymmetric. Of the 21 noncentrosymmetric classes, 20 display piezoelectricity and of these only 10 permit the existence of pyroelectricity.²⁸

Because of their special chemical and morphological structures, these crystals possess spontaneous polarization. The variation of spontaneous polarization as a function of temperature is called pyroelectricity. The pyroelectric coefficient (p) of a material can be expressed by Eqn [1].

$$i = Ap \, dT/dt \quad [1]$$

where dT/dt is the rate of change of temperature, i is the electric current and A is the cross-sectional area of the material. In pyroelectrics, if the direction of spontaneous polarization can be reversed by an applied external electric field, then they are known as ferroelectrics. The electrical charge generated in a material by applied mechanical stress is called piezoelectricity. Ferroelectric materials display pyro- and piezo-electric effects. Therefore, a polar material may have three different electronic functions. On a symmetry basis, the absence of a center of symmetry is a necessary condition to show piezoelectricity.

Pyro-, piezo and ferro-electric properties have been studied in organic molecular and polymeric materials including biomaterials. Poly(vinylidene fluoride), PVDF, is the only known polymer so far that shows pyro-, piezo-, and ferro-electric properties. PVDF has a chemical structure

$-(CH_2CF_2)_n-$, consisting of highly polar carbon-fluorine bonds. Other ferroelectric polymers include copolymers and blends of PVDF, some nylons such as nylon-11, nylon-9 and nylon-5,7, and vinylidene cyanide copolymers. For more detailed studies on pyro-, piezo- and ferro-electric effects in organic polymers, readers are referred to a recent review on the subject.¹⁹

Electrical properties such as dielectric constant, dielectric loss, dielectric breakdown, pyroelectricity and piezoelectricity have been reported in organic LB films. The temperature dependence of dielectric breakdown in LB films of the barium salts of fatty acids was shown by Agarwal and Srivastava.²⁹ The correlation of thickness with dielectric constant of LB films of barium palmitate, stearate and behenate was investigated by Kapur and Srivastava.³⁰

Polar structures can be easily built-up by the LB technique. The first report on pyroelectricity in LB films of a series of amphiphilic azoxy compounds appeared in 1982.³¹ The pyroelectric coefficient in ω -tricosenoic acid/docosylamine alternate LB films (99-layer) was found to be $1 \times 10^{-9} \text{ C cm}^{-2} \text{ K}^{-1}$.³² LB films of a 2:1 mixture of 4-cyano-4'-pentyl-*p*-terphenyl with cadmium arachidate exhibit a pyroelectric coefficient of $1 \times 10^{-10} \text{ C cm}^{-2} \text{ K}^{-1}$ at room temperature.³³ Piezoelectric effects in noncentrosymmetric multilayers of 4-nitro-4'-octadecylazobenzene were reported by Novak and Myagkov.³⁴

Organometallic materials have rarely been explored in connection with pyro-, piezo-, and ferro-electric properties; therefore there are only a few reports on organometallic LB films. A group at Oxford has studied pyroelectric properties of organoruthenium complexes. Roberts *et al.*^{35,36} reported the pyroelectric properties of LB films of ruthenium (η^5 -cyclopentadienyl)(bistriphenylphosphine) derivatives. Figure 6 shows the molecular structures of these ruthenium compounds. The static pyroelectric coefficients for alternate layer structures of the ruthenium complexes with behenic acid were -0.01 , -0.04 , -0.25 , -0.45 , and $0.5 \mu\text{C m}^{-2} \text{ K}^{-1}$ for the ruthenium compounds **II**–**VI** respectively. The pyroelectric coefficient decreases as the number of phenyl rings increases and, as a result, ruthenium complex **VI** showed the largest and complex **II** the lowest value for the pyroelectric coefficient.

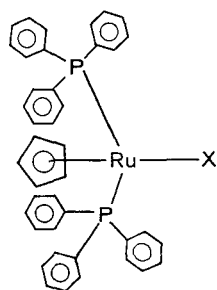
The pyroelectric coefficients were also measured for multilayers of behenic acid alternated with mixtures of ruthenium complex **VI**. The

pyroelectric coefficient varies with composition and a mixture of 70% of ruthenium complex **VI** and 30% behenic acid showed the highest pyroelectric coefficient of $-3.0 \mu\text{C m}^{-2} \text{K}^{-1}$. Relative permittivity and dielectric loss of a ruthenium complex/behenic acid alternate layer structure as a function of temperature and frequency were also reported. For thermal imaging applications, the low dielectric loss and relative permittivity yields a figure of merit of $0.8 \mu\text{C cm}^{-2} \text{K}^{-1}$ at room temperature for the ruthenium complex LB film superlattice at a scale where poly(vinylidene fluoride) has a figure of merit of $2.7 \mu\text{C cm}^{-2} \text{K}^{-1}$. The LB film has a dielectric loss, $\tan \delta$ of 0.03 at a frequency of 100 Hz at 25°C . The pyroelectric properties of LB superlattices were found to be affected by the structural quality of the films, their ionic nature and dipole moments.³⁷

Pyroelectric coefficients as high as $2.7 \mu\text{C m}^{-2} \text{K}^{-1}$ were achieved by improving the structural quality of the LB film. LB films of the organoruthenium complex [cyclopentadienyl (bistriphenylphosphine) ruthenium(4-hepta-decyloxybenzonitrile) hexafluorophosphate] alternating with behenic acid have superior structural stability and display large pyroelectric responses.³⁸ The dielectric and pyroelectric properties and the figure of merit indicate appli-

cability of organoruthenium LB films in thermal imaging devices.

Ruthenium complex LB films also exhibit interesting electrochemistry and chemiluminescence properties. Electrode modification by LB films of surfactant derivatives of $\text{M}(\text{bpy})_3^{2+}$ ($\text{M} = \text{Ru}, \text{Os}$; $\text{bpy} = 2,2'$ -bipyridine) have been investigated. The LB films of ruthenium and osmium derivatives transferred to tin oxide (SnO_2) electrodes at 20 mN m^{-1} showed a voltammetric wave with E_{fwhm} near 100 mV .³⁹ Miller *et al.* studied the electrochemistry and subsequent trough electro-generated chemiluminescence (ECL) photography of Langmuir monolayers of luminescent ruthenium complexes.^{40,41} Figure 7 shows the chemical structures of $\text{Ru}(\text{bpy})_2(\text{bpy}-\text{C}_{19})^{2+}$ and $\text{Ru}(\text{dp-bpy})_3^{2+}$. The monolayers of $\text{Ru}(\text{bpy})_2(\text{bpy}-\text{C}_{19})^{2+}$ and $\text{Ru}(\text{dp-bpy})_3^{2+}$ were transferred onto a highly oriented pyrolytic graphite (HOPG) electrode at a surface coverage of 110 and $125 \text{ \AA}^2 \text{ molecule}^{-1}$ respectively. The ECL intensity of the $\text{Ru}(\text{bpy})_2(\text{bpy}-\text{C}_{19})^{2+}$ monolayer was about two orders of magnitude larger than that of the $\text{Ru}(\text{dp-bpy})_3^{2+}$ monolayer. ECL photography of ruthenium complex monolayers transferred onto HOPG and ITO electrodes showed that aggregation of the amphiphiles takes place at very low or zero surface pressure prior to their compression. By using nanosecond laser photolysis, electron transfer quenching of excited pyrene or $\text{Ru}(\text{II})(\text{bpy})_3^{2+}$ in LB films by donor or acceptor surfactant molecules with different redox potentials was also studied.⁴² $\text{Ru}(\text{II})(\text{bpy})_3^{2+}$ having two alkyl chains ($\text{Ru}-\text{C}_{15}$) and ($\text{Ru}-\text{C}_{19}$) (Figure 8) and 10-(1-pyrene)decanoic acid were used as sensitizers. Derivatized pyridinium, anthraquinone, viologen and TCNQ surfactants were used as acceptors and a ferrocene surfactant as a donor. The redox potential of four acceptors and one donor ranges to 1.8 V width. Monolayer characteristics of sensitizers, acceptors, and donor amphiphiles, and the luminescence lifetime of the sensitizer in LB films, were reported.



1. $\text{X} = \text{PF}_6^- \text{N}^+ \equiv \text{C} - \text{C}_6\text{H}_4 - \text{C}_6\text{H}_4 - \text{C}_6\text{H}_4 - \text{C}_5\text{H}_{11}$
2. $\text{X} = \text{PF}_6^- \text{N}^+ \equiv \text{C} - \text{C}_6\text{H}_4 - \text{C}_6\text{H}_4 - \text{C}_{12}\text{H}_{25}$
3. $\text{X} = \text{PF}_6^- \text{N}^+ \equiv \text{C} - \text{C}_6\text{H}_4 - \text{C}_{12}\text{H}_{25}$
4. $\text{X} = \text{PF}_6^- \text{N}^+ \equiv \text{C} - \text{C}_6\text{H}_4 - \text{O} - \text{C}_{12}\text{H}_{25}$
5. $\text{X} = \text{PF}_6^- \text{N}^+ \equiv \text{C} - \text{C}_6\text{H}_4 - \text{O} - \text{C}_{17}\text{H}_{35}$

Figure 6 Molecular structures of organoruthenium complexes 1 = **II**, 2 = **III**, 3 = **IV**, 4 = **V**, and 5 = **VI** (after Refs 35, 36).

3.2 Electrically conducting organometallic LB films

The electrical conductivity (σ) of a material is measured in units of S cm^{-1} ($= \Omega^{-1} \text{ cm}^{-1}$) and can be simply expressed by Eqn [2]:

$$\sigma = ne\mu \quad [2]$$

where n is the number-density of the charge

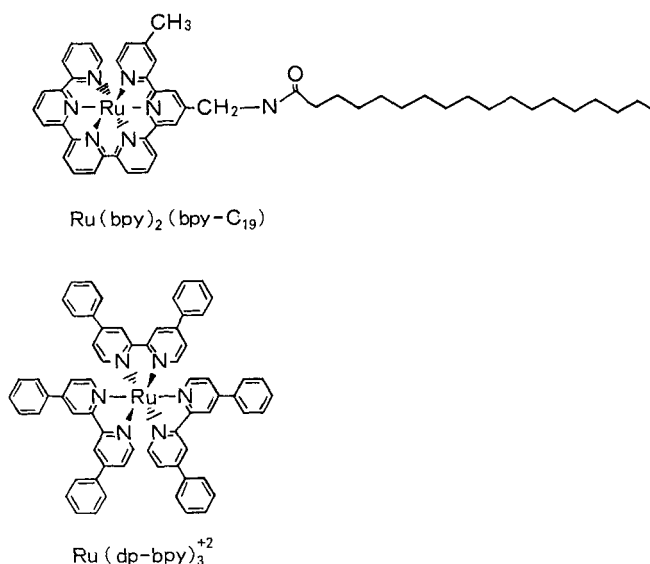


Figure 7 Chemical structures of $\text{Ru}(\text{bpy})_2(\text{bpy}-\text{C}_{19})$ and $\text{Ru}(\text{dp-bpy})_3^{2+}$ compounds (after Refs 40, 41).

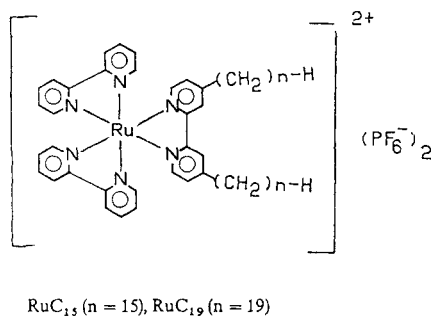
carriers in cm^{-3} , e is the electronic charge of the carriers in coulombs, and μ is the mobility of the charge carriers in $\text{cm}^2 \text{V}^{-1} \text{s}^{-1}$. From this equation, it is apparent that the conductivity is directly proportional to the number-density of the charge carriers, electrons and/or holes and their mobility. Therefore, high conductivity can be achieved by generating a high concentration of charge carriers.

Electrical conductivity can be of two types: intrinsic conductivity, which is the property of a material and is related to the electronic state characteristics, and extrinsic conductivity, which is associated with foreign moieties such as impurities or doping in the material.

High conductivity can be introduced by doping which generates a high density of charge carriers after either oxidation or reduction. The doping species may be either an oxidizing agent or a

reducing agent. Oxidizing agents such as iodine, bromine, arsenic pentafluoride, antimony pentachloride, etc., remove electrons from the π -conjugated system to generate a delocalized cationic species. On the other hand, reducing agents such as sodium metal, sodium naphthalide, etc., donate electrons to the π -conjugated system to yield delocalized, anionic species. Oxidation and reduction processes in π -conjugated systems can be achieved either chemically or electrochemically. Conductivity can be increased from insulating to semiconducting to the metallic regime by doping with electron acceptors or donors.

High mobility of charge carriers can be achieved by an extended π -electron conjugated system where π -electrons are delocalized and can act as charge carriers. In addition, overlapping of π -orbitals can provide a pathway for electronic transport. Organic π -conjugated systems fulfil this criteria. In particular, π -electron conjugation holds the key to high conductivity generated after molecular doping. As shown in Fig. 9, on the basis of electrical conductivity materials can be divided into three classes: insulators having conductivities lower than $10^{-10} \text{ S cm}^{-1}$, semiconductors having conductivities in the range of 10^{-10} to 10^2 S cm^{-1} , and metals possessing conductivities higher than 10^2 S cm^{-1} . The electrical conductivity of materials spans more than 24 orders of magnitude from a good insulator to a superconductor. Organometallic LB films exhibit conductivities up to the metallic regime, as will be later mentioned in the text.



RuC_{15} ($n = 15$), RuC_{19} ($n = 19$)

Figure 8 Chemical structures of $\text{Ru}(\text{dp-bpy})_3^{2+}$ compound having two alkyl chains (after Ref. 42).

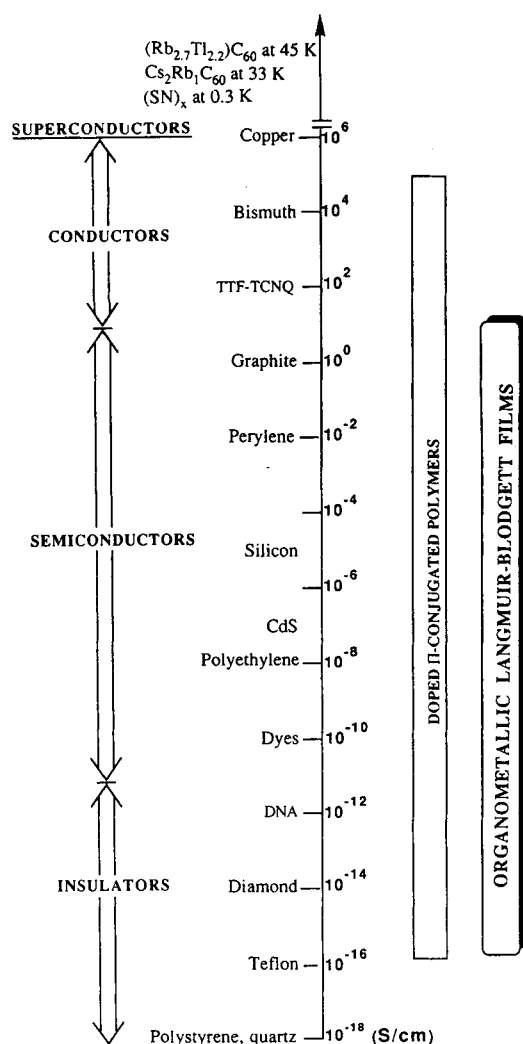


Figure 9 Conductivity scale of various materials along with the conductivity range of organometallic LB films.

Two classes of π -conjugated materials, viz. organic charge-transfer complexes and π -conjugated polymers, have been extensively explored over the past decade. Custom-made organic molecules that exhibit metallic conductivity are known as 'synthetic metals'. It is the temperature dependence of conductivity that decides whether a material is semiconducting or metallic. In these synthetic metals, electrical conductivity increases as the temperature decreases. Tetrathiafulvalene (TTF)-tetracyano-*p*-quinodimethane (TCNQ) is one example of an electrically conducting charge-transfer complex that contains both cation and anion radicals in a 1:1 ratio.⁴³ The tetramethyltetraselenafulvalenium (TMTSF) salt, (TMTSF)₂PF₆, is the

first example of an organic superconductor ($T_c = 0.9$ K at $P = 12$ kbar).⁴⁴ Besides TMTSF, organic superconductors based on BEDT-TTF, MDT-TTF, BEDO-TTF, DMET and the [M(dmit)₂]⁻ anion have been developed.⁴⁵⁻⁴⁸ Examples of π -electron conjugated polymers are polyacetylene, polypyrrole, polythiophene, poly(*p*-phenylene), poly(*p*-phenylene vinylene), poly(*p*-phenylene sulfide), polycarbazole, polyisothianaphthene, polyaniline, and hetero-aromatic ladder polymers. Polyacetylene is the prototype electrically conducting organic polymer possessing a one-dimensional π -electron conjugated backbone. Polyacetylenes, upon iodine doping, show the conductivities as high as that of copper metal. In the case of poly(*p*-phenylene), the conductivity increases by 18 orders of magnitude from 10⁻¹⁶ to 500 S cm⁻¹ upon doping with arsenic pentafluoride.⁴⁹

Several conduction mechanisms have been suggested to describe organic conducting materials.^{50,51} A theoretical model of Mott's variable range hopping (VRH) conduction can predict transport processes in disordered semiconducting materials.⁵² The conductivity (σ)-temperature (T) data are plotted as $\log \sigma$ versus T^{-x} , where x is a constant ranging from 1 to $\frac{1}{4}$. The $x = \frac{1}{2}$, $\frac{1}{3}$ and $\frac{1}{4}$ behavior evidences pseudo-one-dimensional, two-dimensional, and three-dimensional conduction processes, respectively. Therefore, from $\log \sigma$ versus T^{-x} dependence a conduction mechanism can be evaluated. In conjugated polymer solids, solitonic and bipolaronic conduction mechanisms have been proposed.^{53,54} It is likely that organometallic materials will also show high electrical conductivities and this is a rapidly growing field of current research. In organic conjugated polymers, metallic-like conductivity is generated by a molecular doping process whereas organometallic polymers may act as intrinsic conductors. A comprehensive, detailed description of electrically conducting organometallic polymers has recently been presented by Nalwa in this Journal.⁵⁵ Electrically conducting polymers⁵⁶ and their promising applications⁵⁷ in a variety of electronic technologies have been described in reference texts. Some of these π -conjugated polymers such as polythiophenes, polypyrroles, polyanilines, poly(*p*-phenylene vinylene), etc., form electrically conducting LB films.

A wide variety of π -electron conjugated molecules has been chemically tailored into LB molecules to study their electrical properties. For more

details on conducting LB films the reader is referred to the literature referenced below. Electrically conducting LB films were reviewed by Nakamura and Kawabata⁵⁸ and Tieke.⁵⁹ This topic has also been discussed in reference texts by Ferraro and Williams,⁶⁰ and Ulman.⁶¹ Table I lists the electrical conductivity of organic materials that were studied by developing LB monolayers and multilayers.⁶²⁻⁷⁶ Electrical conductivities of the LB films of four types of organic conjugated materials were summarized: (1) anion radical

salts; (2) cation radical salts; (3) charge-transfer complexes; and (4) polymers. The conductivities of LB films range from 5.0 to $10^{-6} \text{ S cm}^{-1}$, depending upon the type of the conjugated material, charge-transfer formation, and doping procedure. The magnitude of conductivity in these materials can be viewed as moderate since their conductivities remain in a semiconducting regime. We focus our attention here on organo-metallic LB films, a new class of material where charge-transfer interactions between the metal

Table I Electrical conductivities of LB films of organic π -conjugated materials after doping

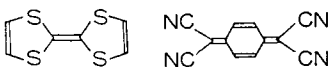
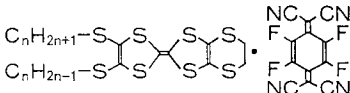
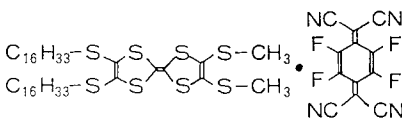
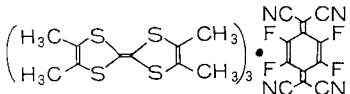
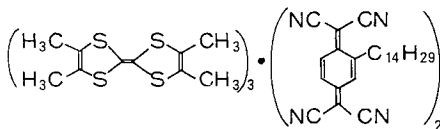
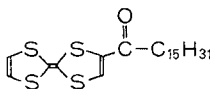
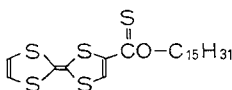
LB material		Abbreviation	$\sigma (\text{S cm}^{-1})$	Ref.
Structure				
		TTF-TCNQ	5.5	62
		$\text{C}_{16}\text{TET-TTF-F}_4\text{TCNQ } (n=16)$	0.25^a	63
		$\text{C}_{18}\text{TET-TTF-F}_4\text{TCNQ } (n=18)$	0.01^a	64
		$\text{C}_{16}\text{TDMT-TTF-F}_4\text{TCNQ}$	10^{-3}^a	64
		TMTTF- F_4TCNQ	1.0	62
		TMTTF- C_{14}TCNQ	0.1	65
		C_{16}TTF	0.01^a	66
		C_{16}OTTF	1.0^b	67

Table 1 *Continued*

LB material			
Structure	Abbreviation	σ (S cm ⁻¹)	Ref.
	C ₈ TTT	0.01 ^a	68
	TTT-CF ₃	1.2 × 10 ^{-4a}	68
	C ₁₈ PyTCNQ ($n = 18, m = 1$)	0.01 ^a	69
	C ₁₈ Py(TCNQ) ₂ ($n = 18, m = 2$)	0.03	70
	C ₂₂ PyTCNQ ($n = 22, m = 1$)	0.01	71
	C ₂₂ Py(TCNQ) ₂ ($n = 22, m = 2$)	0.01	72
	C ₁₈ Py	0.01	73
	P-BT	5.0	74
	C ₁₈ OAn	10 ^{-6a}	75
	PPV	0.5 ^b	76
	β -Apo-8'-carotenoate	6.4 × 10 ^{-6a}	68

^a Iodine doping. ^b SO₃ doping. ^c Deposited from KI₃ subphase and doped with iodine.

ions, and conjugated ligands play an important role. The π -electron conjugated systems in molecules such as phthalocyanines, porphyrins, dithiolenes, annulenes and charge-transfer species are examples of electrically conducting molecular materials. They exhibit metallic characteristics upon doping with electron acceptor or donor species.

3.2.1 Metallophthalocyanines

Only a few reports on the electrical conductivity of organometallic LB films have appeared so far. The conjugated phthalocyanine (Pc) system has 18 electrons in the macrocycle and can accommodate a variety of metal atoms. Furthermore, many peripheral substituents are possible; hence chemical architecture offers a variety of metallophthalocyanines. Nichogi *et al.*⁷⁷ reported the formation of LB films of tetrasubstituted lead phthalocyanine (PcPb) and the effect of substituent groups on the electrical properties. Three PcPb derivatives, viz. tetra(*t*-butyl)phthalocyanine lead (TTBPcPb), lead tetracumylphenoxyphthalocyanine (TCPcPb) and lead tetraphenoxyphthalocyanine (TPOPcPb) were prepared. The structure of these PcPb derivatives are shown in Fig. 10. The LB films were prepared on quartz substrates. The thickness of the LB films was 50–150 nm. All the deposited LB films were of the Z-type. Table 2 lists zero-pressure-extrapolated area, film thickness and conductivity of these LB monolayers. Scanning electron microscopy (SEM) showed microcrystals (2000–3000 nm) in TCPcPb LB films, while TTBPcPb and TPOPcPb LB films surfaces were found to be uniform and smooth. In particular, TPOPcPb showed the largest anisotropy and the high conductivity attributed to the formation of one-dimensional face-to-face stacks. Each LB film exhibited different molecular orientation and conductivities depending upon the nature of the substituents.

Brynda *et al.*⁷⁸ reported the preparation of LB

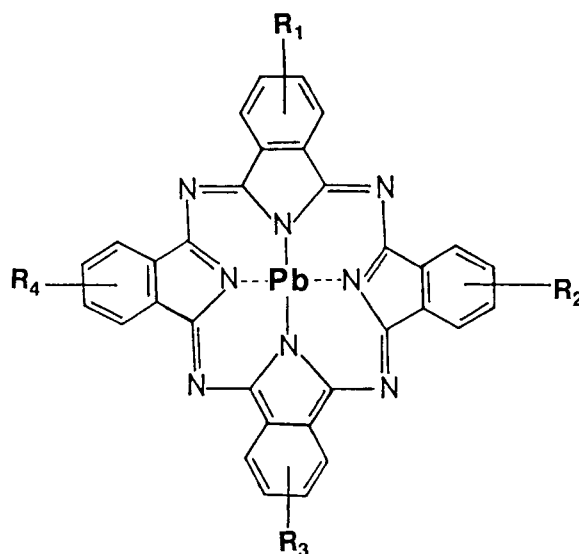


Figure 10 Chemical structure of lead phthalocyanine derivatives. **VII** TTBPcPb: $R_1 = R_2 = R_3 = R_4 = -C(CH_3)_3$; **VIII** TCPcPb: $R_1 = R_2 = R_3 = R_4 = -\text{cumylphenoxy}$; **IX** TPOPcPb: $R_1 = R_2 = R_3 = R_4 = -OC_6H_5$ (after Ref. 77).

films of copper tetra[4(*t*-butyl)phthalocyanine] (CuTTBPc). Monolayers of CuTTBPc were spread from a xylene solution on a water subphase at 17 °C. The CuTTBPc molecule has a surface area of 0.6 nm². The phthalocyanine rings in the LB films were tilted at an angle of 14° to the substrate. The electrical conductivity of CuTTBPc was found to be time-dependent and increased with time to a value of 0.1 S cm⁻¹. A photovoltaic cell constructed from a Al/CuTTBPc LB film/Ni sandwich sample showed an open-circuit voltage of 0.4 V.

Snow *et al.*⁷⁹ reported electrical conductivity and piezoelectric mass measurements on mixed mono- and multi-layer LB films of tetrakis(cumylphenoxy)phthalocyanine compounds (Fig. 11) and octadecanol (stearyl alcohol). Simultaneous measurements of electrical conductivity of LB films and mass change during iodine doping were

Table 2 Zero-pressure-extrapolated (ZPE) area, film thickness and conductivities of tetra-substituted phthalocyanine lead derivatives (after Ref. 77)

LB material	ZPE area (nm ²)	Thickness of monolayer (nm)	Conductivity (S cm ⁻¹)	
			σ_{\parallel}	σ_{\perp}
TTBPcPb	0.662	1.5	$< 3 \times 10^{-10}$	5.0×10^{-12}
TCPcPb	0.386	—	1.1×10^{-11}	8.5×10^{-12}
TPOPcPb	0.765	2.0	3.7×10^{-4}	5×10^{-11}

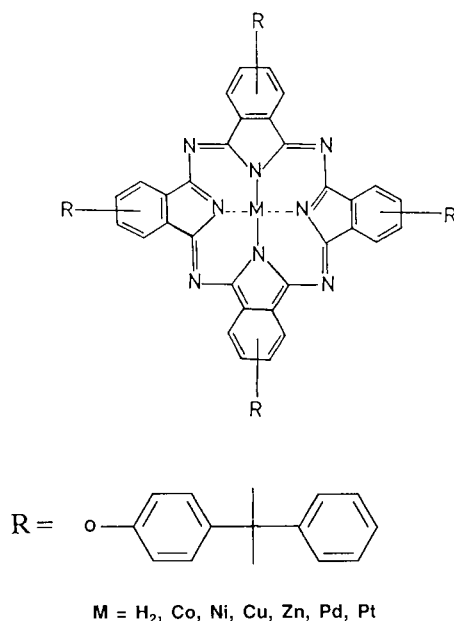


Figure 11 Molecular structure of tetrakis(cumylphenoxy)-metallophthalocyanines. The cumylphenoxy groups are at either the 2- or the 3-positions of the phenyl ring of the macrocycle (after Ref. 79).

performed using a dual 52-MHz surface acoustic wave (SAW) device. Table 3 lists the electrical conductivity of iodine-doped LB films (45 layers) of metal-free, copper, zinc, platinum, palladium, cobalt and nickel phthalocyanine-stearyl alcohol ($C_{18}H_{37}OH$). The conductivity increases by four orders of magnitude from 10^{-10} to $10^{-6} S cm^{-1}$ as the stoichiometric ratio reaches iodine/phthalocyanine = 2:1. The variation of the central metal ion showed little effect on either the increases in the magnitude of the conductivity or the complex stoichiometry. The ratio of moles of absorbed iodine to moles of phthalocyanine ring, X , was calculated by using the proportionality between

SAW frequency shift and film mass and the relative concentration of the phthalocyanine and stearyl alcohol LB film components. A relationship between LB film thickness and microelectrode thickness was also observed. The conductivity increases with increasing multilayer film thickness and saturates as the film thickness became greater than the planar interdigital microelectrode. The magnitude of electrical conductivity increase was found to be independent of the morphology.

Barger *et al.*⁸⁰ reported the preparation of LB films of tetraphenoxy ($-OC_6H_5$), dicumylphenoxy and tetracumylphenoxy ($-OC_6H_4C(CH_3)_2C_6H_5$), tetraoctadecoxy ($-O(CH_2)_{17}CH_3$) and tetraneopentoxy ($-OCH_2C(CH_3)_3$) phthalocyanines. The preparation of chemiresistors of metal-substituted tetracumylphenoxy phthalocyanines $MPc(CP)_4$ containing iron, cobalt, nickel, copper, zinc, palladium, platinum and lead with octadecanol was investigated. The change in electrical conductivity of the chemiresistors prepared with 45-layer LB films was determined on exposure to vapors of ammonia (2 ppm), sulfur dioxide (20 ppm) and dimethyl methyl phosphonate (2 ppm). In particular, NH_3 showed the strongest effect with $MPc(CP)_4$ containing metals of the d_8 and d_9 electron configuration, i.e. nickel, palladium, platinum and copper.⁸¹ Pace *et al.*⁸² reported LB films of metal-free and metal-substituted tetrakis(cumylphenoxy)-phthalocyanine. Oxovanadium-tetakis(cumylphenoxy)phthalocyanine ($VOPcX_4$) and copper-tetrakis(cumylphenoxy)phthalocyanine ($CuPcX_4$) showed similar packing arrangements with an order parameter of -0.45 . Iodine doping of $VOPcX_4$, $CuPcX_4$, and H_2PcX_4 LB films demonstrated that the electron spin resonance (ESR) signal is related to conductivity and to the quantity of iodine absorbed. The $VOPcX_4$ film showed

Table 3 Electrical conductivity of LB films of tetrakis(cumylphenoxy)-phthalocyanine compounds and $C_{18}OH$ (after Ref. 79)

MPcCP	Conductivity, $\sigma(S cm^{-1})$		Ratio of absorbed iodine to phthalocyanine ring, X
	Undoped	Iodine-doped	
$H_2Pc(CP)_4$	2×10^{-9}	6×10^{-6}	2.2
$CuPc(CP)_4$	6×10^{-10}	6×10^{-6}	2.2
$ZnPc(CP)_4$	2×10^{-10}	3×10^{-6}	2.0
$PtPc(CP)_4$	2×10^{-11}	3×10^{-6}	2.5
$PdPc(CP)_4$	3×10^{-10}	1×10^{-6}	3.9
$CoPc(CP)_4C$	8×10^{-10}	1×10^{-6}	2.6
$NiPc(CP)_4$	8×10^{-11}	63×10^{-7}	2.8

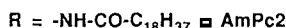
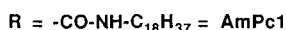
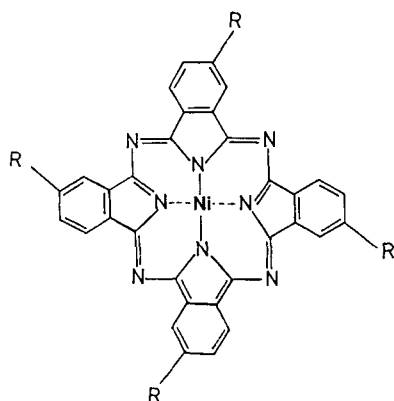


Figure 12 Nickel phthalocyanine containing long alkyl-chain amide groups (after Ref. 83).

a g -value of 1.9951. Iodine doping of a thin film (45 layers) of H_2PcX_2 and strearyl alcohol composition showed significant increase in conductivity by four orders of magnitude from 10^{-10} to $10^{-6} \text{ S cm}^{-1}$ during the first 600 s of doping. The conductivity of complexed transition-metal ions themselves were not reported but little effect was anticipated.

Fujiki *et al.*⁸³ described two highly soluble nickel phthalocyanine complexes containing four long-chain alkyl amides (their structures are shown in Fig. 12): $-\text{CONH}-\text{C}_{18}\text{H}_{37}$ and $-\text{NHCO}-\text{C}_{18}\text{H}_{37}$, referred to as AmPc1 and AmPc2, respectively. The LB films of AmPc1 were prepared by the vertical dipping technique, that of AmPc2 by the horizontal lifting method. Table 4 lists the electrical conductivities of the undoped and iodine-doped AmPc1 and AmPc2 LB films. With iodine doping, conductivity increases by two and four orders of magnitude for AmPc2 and AmPc1, respectively. The conductivity values of the undoped as well as of doped LB films were higher than those of spin-cast films.

Fujiki and Tabei⁸⁴ reported the electrical properties of LB films of MPcs ($M = \text{Ni}, \text{Cu}, \text{Pb}$ and H_2) containing short substituents such as tert-butyl (TB), isopropyl (IP), and cyano (C) groups (Fig. 13). The LB films were prepared by the horizontal lifting technique. The limiting surface areas of TBPC M , where M is Ni, Cu and H_2 , were $32\text{--}43 \text{ \AA}^2 \text{ molecule}^{-1}$. TBPCPb did not yield reproducible force-area isotherms due to its

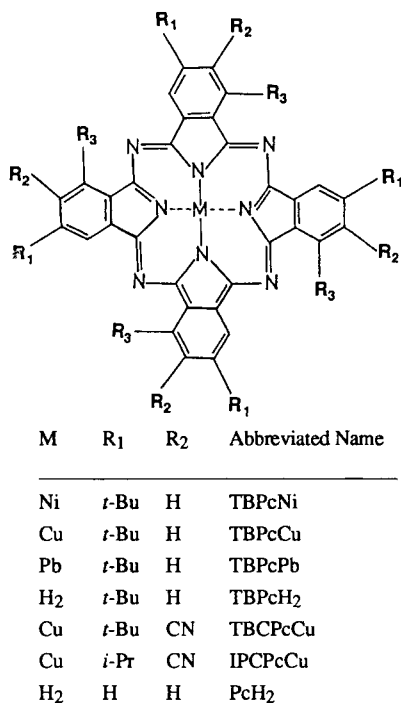
decomposition at the water-air interface and was less stable towards heat, light and water. The surface areas of TBPCCu and IPCPCu were 0.69 and $0.75 \text{ nm}^2 \text{ molecule}^{-1}$, respectively. Table 5 lists the in-plane conductivities of undoped and doped LB films (film thickness, *ca* 0.80 nm) with active gases such as iodine and triethylamine at room temperature. Undoped LB films have conductivities of the order of 10^{-8} to $10^{-9} \text{ S cm}^{-1}$. The conductivities of undoped LB films containing cyano groups were found to be highly sensitive and reversible. Iodine doping increases the conductivity by five orders of magnitude; PcH_2 LB films showed the greatest value of $10^{-3} \text{ S cm}^{-1}$. Electron-donating triethylamine increased conductivity by 2–400 times within 20–30 s of exposure to the gas. Similarly, *n*-butanethiol, which also donates electrons, raised conductivity by 600–3000 times, where TBPCu and TBPCCu on doping showed conductivities of 5.0×10^{-6} and $3.8 \times 10^{-6} \text{ S cm}^{-1}$, respectively. The magnitude of the conductivity and the response of the LB films to the active gases were related to the estimated ionization potentials and electron affinities of the films.

Gupta *et al.*⁸⁵ described LB films of a bridged variety in μ -oxo-bis[tetra(*t*-butyl)phthalocyanine iron(II)], referred to as $(\text{FeTBPC})_2\text{O}$ (Fig. 14). The LB monolayers of $(\text{FeTBPC})_2\text{O}$ were deposited at a surface pressure of 35 mN m^{-1} from a xylene solution at a temperature of 25°C and pH of 6.0. The surface pressure-area isotherm showed an extrapolated area per molecule of 1.66 nm^2 . The deposited film showed an optical absorption maximum (λ_{max}) at 656 nm . The conductivity of the freshly prepared LB film was $4.0 \times 10^{-4} \text{ S cm}^{-1}$ and there was a 20% reduction in conductivity following vacuum pumping. Doping with ammonia decreased conductivity further by 30% at high concentration. Iodine doping raised the conductivity of these LB films by 80%. The activation energy of 10.6 kJ mol^{-1} was derived from conductivity-temperature plots. Hann *et al.*⁸⁶ reported a conductivity of $1.0 \times 10^{-4} \text{ S cm}^{-1}$ for the corresponding mononuclear complex of copper(II), CuTBP multilayers and an activation energy of 18.3 kJ mol^{-1} .

Roberts *et al.*⁸⁷ showed that the solvent plays a role in the preparation of LB monolayers of phthalocyanines. The LB films obtained from tetra(*t*-butyl)zinc phthalocyanine from chloroform-xylene, tetra(*t*-butyl)copper phthalocyanine from xylene, tetra(*t*-butyl)manganese phthalocyanine from xylene-dimethylformamide

Table 4 In-plane conductivity of the AmPc1 and AmPc2 LB films (after Ref. 83)

NiPc	LB mode	Conductivity (S cm ⁻¹)	
		Undoped	Iodine-doped
—CONH—C ₁₈ H ₃₇	Y-type (20 layers)	(0.8–8) × 10 ⁻¹⁰	(0.8–2) × 10 ⁻⁶
—NHCO—C ₁₈ H ₃₇	X-type (10 layers)	(4–7) × 10 ⁻⁸	(0.7–2) × 10 ⁻⁶

**Figure 13** Metallophthalocyanines with short substituents (after Ref. 84).

and of asymmetric copper phthalocyanine from chloroform exhibited areas per molecule of 0.92, 0.87, 0.86 and 0.57 nm², respectively. The conductivity of asymmetric CuPc was approx.

10⁻⁸ S cm⁻¹. Electronic devices were prepared by utilizing LB films of these phthalocyanines. Copper tetra(*n*-butoxycarbonyl)phthalocyanine derivatives also form highly ordered monolayer assemblies.⁸⁸

Palacin *et al.*⁸⁹ studied mixed monolayer formations of an amphiphilic vanadyl tetraoctadecyl tetrapyrindino[3,4-*b*:3',4'-*g*:3'',4''-*l*:3''',4'''-*q*]porphyrinium bromide (VOS₁₈Br₄) (Fig. 15) and stearic acid. The amphiphile has an area per chain between 0.22 and 0.25 nm² and attains an ordered structure. A reaction between VOS₁₈Br₄ and stearic acid takes place in the monolayer phase, causing some reorganization. The electrostatic attraction between the pyridinium rings and the stearate ion holds the single-chain molecule close to the microcycle; this allows good control of the in-plane coupling between the metal ions.

Kalina and Crane⁹⁰ described the preparation of LB films of copper octa(dodecyloxy-methyl)phthalocyanine. From the pressure–area isotherm, an area of 1.80 nm² molecule⁻¹ was estimated. Monolayers could be transferred onto various substrates up to 150 layers in thickness from the trough. Some degree of molecular aggregation was observed for LB films deposited on ITO coated glass.

Electronic states and the charge-transfer mechanism in the monolayers of tetra(octadecyl-aminosulfanyl) vanadyl phthalocyanine were investigated by Solinsh *et al.*⁹¹

Table 5 Estimated ionization potential (*I*_p), electron affinity (*E*_A), and in-plane electrical conductivity of LB films of substituted MPCs (after Ref. 84)

Pc compound	<i>I</i> _p (kJ mol ⁻¹)	<i>E</i> _A (kJ mol ⁻¹)	Conductivity (S cm ⁻¹)		
			Undoped	Iodine	Triethylamine
TBPcNi	473	280	5.7 × 10 ⁻⁸	2.5 × 10 ⁻⁴	1.2 × 10 ⁻⁷
TBPcCu	478	275	1.5 × 10 ⁻⁹	3.4 × 10 ⁻⁵	1.7 × 10 ⁻⁷
TBPcH ₂	497	304	3.8 × 10 ⁻⁸	5.4 × 10 ⁻⁴	1.2 × 10 ⁻⁷
TBCPcCu	526	338	7.6 × 10 ⁻⁹	3.4 × 10 ⁻⁴	2.9 × 10 ⁻⁶
IPCPcCu	526	338	4.0 × 10 ⁻⁹	4.6 × 10 ⁻⁶	8.0 × 10 ⁻⁷
PcH ₂	502	309	2.9 × 10 ⁻⁸	2.6 × 10 ⁻³	6.0 × 10 ⁻⁷

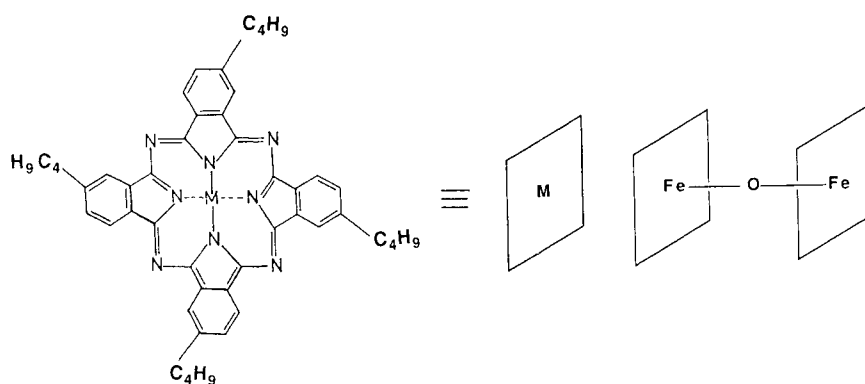


Figure 14 Chemical structure of a monomeric μ -oxo-bis[tetra-*t*-butylphthalocyanine iron(II)] (FeTBPO)₂O (a) and a dimeric phthalocyanine (b) (after Ref. 85).

Orthmann and Wegner⁹² reported the preparation of ultrathin films of substituted phthalocyanato-polysiloxane (Fig. 16) by the LB technique. The applications of these LB films in chemical sensors were demonstrated.⁹³ Ali-adib *et al.*⁹⁴ reported the magnetic orientation of phthalocyanato-polysiloxanes. Octa-substituted monomers of silicon dichloride- and silicon dihydroxy-phthalocyanines having alkyl chains of uniform length to the periphery of each phthalocyanine ring were synthesized. From them were obtained phthalocyaninato-polysiloxanes having all-butoxy or all-decyloxy side chains. The phthalocyanine monomer, with an $\text{Si}(\text{OH})_2$ group at the center of the macrocycle having butoxy side-

groups, has a surface area of approx. 2.6 nm^2 . Its isotherm was quite different from that of decyloxy-substituted phthalocyanine. The monolayers of polymers of both butoxy- and decyloxy-substituted phthalocyanine were deposited as Y-type. The butoxy- and decyloxy-substituted polymers showed surface areas of about 1.6 and 1.3 nm^2 , respectively. Films of the polymers cast from solution in a magnetic field of 5 T gave a dichroic ratio of up to 7.3 at 555 nm . The application of a magnetic field during casting leads to more perfect orientation and, as a result, a higher dichroic ratio was obtained compared with the LB technique.

Lanthanide bisphthalocyanines have been considered important because of their unique electrochromic and semiconducting properties. As a result, LB films of phthalocyanine complexes of lanthanides ($4f$ elements) are attracting attention. Mixed monolayers of ytterbium bisphthalocyanine (YbPc_2) and stearic acid were reported by Petty *et al.*,⁹⁵ and (HoPc_2) and (DyPc_2) and arachidic acid mixtures by Souto *et al.*⁹⁶ Recently LB films of lutetium bisphthalocyanine (LuPc_2) and ytterbium bisphthalocyanine (YbPc_2) complexes have been reported.⁹⁷ The limiting surface area for both bisphthalocyanines was *ca* 0.80 nm^2 for edge-on orientation, taking into consideration that the phenyl groups of the neighboring molecules are interlocking. The LB monolayers can be transferred onto glass slides and multilayers were formed from a Z-deposition technique. These bisphthalocyanines form complexes with a gas mixture of nitrogen dioxide ($\text{NO}_2/\text{N}_2\text{O}_4$), as was evidenced by UV/vis and Raman spectroscopy. The gas mixture was chemisorbed onto the LuPc_2 and YbPc_2 films forming a complex that increased the oxidation state of the metal. Spectroscopic

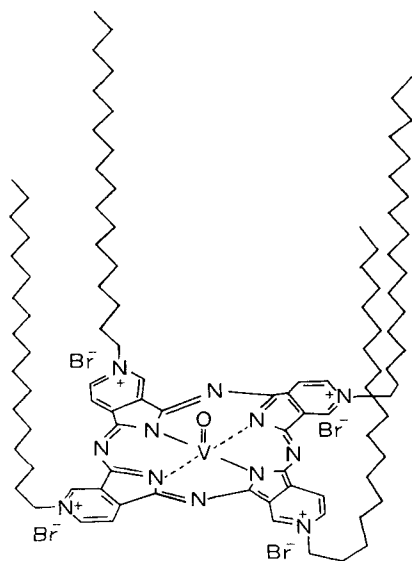


Figure 15 Vanadyl tetraoctadecyl tetrapyridino[3,4-*b*:3',4'-*g*:3'',4''-*l*:3''',4'''-*q*]porphyrizinium bromide ($\text{VOS}_{18}\text{Br}_4$) (after Ref. 89).

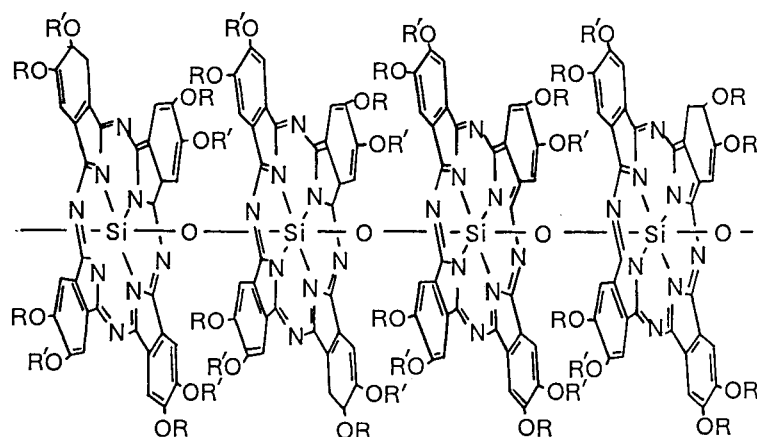


Figure 16 Chemical structure of a phthalocyaninato-polysiloxane ($R = \text{CH}_3$, $R' = \text{C}_8\text{H}_{17}$) (after Ref. 93).

studies of LB monolayers of praseodymium bisphthalocyanines (PrPc_2) and a tetra(*t*-butyl) derivative, $[\text{4-(t-Bu)}_4\text{Pc}]_2\text{Pr}$, have also been reported.⁹⁸ The electron acceptor nitrogen dioxide (NO_2) gas forms complexes with both PrPc_2 and $[\text{4-(t-Bu)}_4\text{Pc}]_2\text{Pr}$. Reversible chemical absorption of NO_2 on the LB monolayer of both complexes was observed.

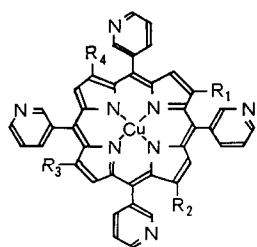
3.2.2 Metalloporphyrins

Like phthalocyanine macrocycles, porphyrins are another π -conjugated system that can accommodate many metal atoms and exhibit unconventional properties. Tredgold *et al.*⁹⁹ studied LB films of copper and silver complexes of mesoporphyrin-IX diol and copper, cadmium, and cobalt complexes of mesoporphyrin-IX dimethyl ester (Fig. 17) and of various fatty acids. In the case of diol derivatives of mesoporphyrin-IX with either arachidic or stearic acid, a well-ordered superlattice structure was obtained having the expected repeat distance, whereas amphiphilic diester derivatives cause the segregation of the porphyrin and the fatty acid into distinct regions. Copper diol and copper diester porphyrins showed in-plane conductivity of 3.4×10^{-5} and $4 \times 10^{-6} \text{ S cm}^{-1}$, respectively. The conductivity of the copper diol and copper diester deposited in alternate layers with arachidic acid were 8.7×10^{-5} and $3 \times 10^{-8} \text{ S cm}^{-1}$, respectively. The conductivity of the LB films containing the diester and arachidic acid was about two orders of magni-

tude lower than that of the pure copper diester. This decrease in conductivity resulted from the segregation of the two materials into separate regions.

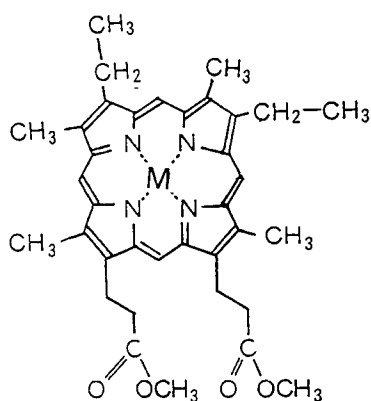
LB films of porphyrins with or without aliphatic chains or porphyrins mixed with phospholipids have been reported by Mohwald *et al.*¹⁰⁰ Homogeneous LB monolayers were formed only for porphyrins having aliphatic chains or in mixtures with lipids. Zinc 3,8-bis(1'-heptadecenyl)deuterioporphyrin dimethyl ester (ZnHDPDME) containing two aliphatic side-chains at one edge of the porphyrin and two hydrophilic ester groups at the opposite edge (Fig. 18) formed an ordered structure. The π - A isotherm showed that pressure increases to above 1 mN m^{-1} at 0.90 nm^2 and above 30 mN m^{-1} at 0.66 nm^2 . A magnesium octaethylporphyrin (MgOEP) did not form any monolayers. The LB films of ruthenium porphyrin dimer (Fig. 19) were reported by Luk and Williams.¹⁰¹ The pressure-area diagram of the ruthenium carbonyl mesoporphyrin-IX pyridate exhibited in an area of $0.60 \text{ nm}^2 \text{ molecule}^{-1}$ in which the porphyrins were stacked perpendicular to the surface. A dimer having a ruthenium-ruthenium (Ru-Ru) bond was obtained by irradiating the monomer films. The *in-situ* preparation of the Ru-Ru porphyrin dimer is interesting for building up co-facially oriented porphyrin moieties linked together through a central metal atom. The LB monolayer and multilayers of a series of porphyr-

ins substituted with cyano groups (structure X–XV) have been reported by McArdle and Ruau-del-Teixier.¹⁰²

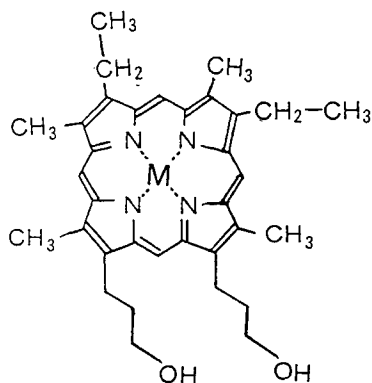


- X** $R_1 = R_2 = R_3 = R_4 = H$
XI $R_1 = R_2 = R_3 = H, R_4 = CN$
XII $R_1 = R_2 = CN, R_3 = R_4 = H$
XIII $R_1 = R_3 = CN, R_2 = R_4 = H$
XIV $R_1 = R_2 R_3 = CN, R_4 = H$
XV $R_1 = R_2 = R_3 = R_4 = CN$

Cyano-substitution causes a change in the



Mesoporphyrin-IX dimethylester



Mesoporphyrin-IX diol

Figure 17 Chemical structures of copper and silver complexes of mesoporphyrin-IX diol and copper, cadmium and cobalt complexes of mesoporphyrin-IX dimethyl ester (after Ref. 99).

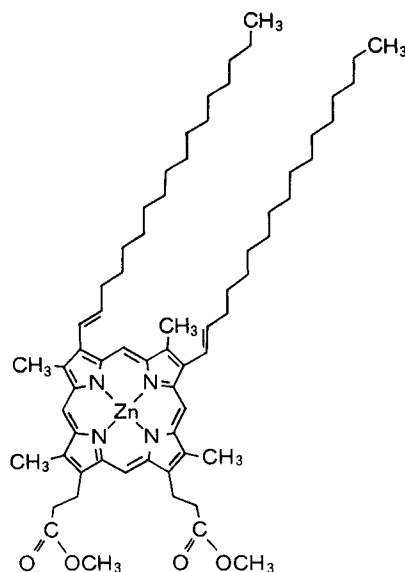


Figure 18 Structure of zinc 3,8-bis(1'-heptadecenyl)deuterioporphyrin dimethyl ester, ZnHDPME (after Ref. 100).

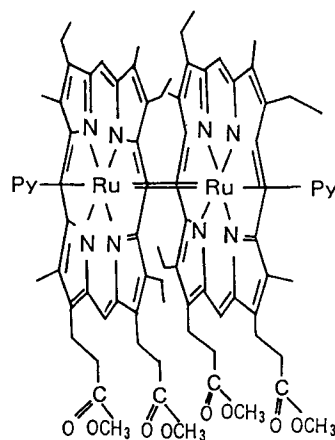
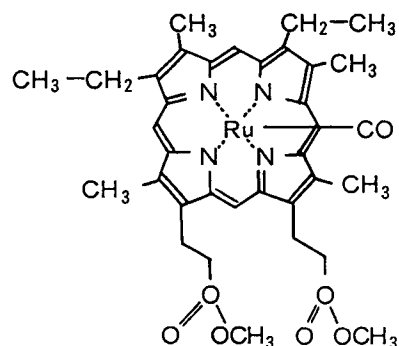


Figure 19 Ruthenium carbonyl mesoporphyrin-IX pyridate (a) and a dimer (b) obtained after photo-irradiation of the monomer (after Ref. 101).

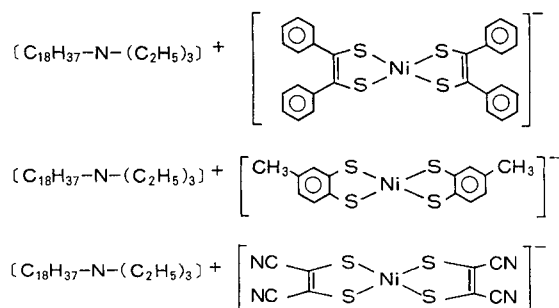


Figure 20 Nickel complexes of long alkylammonium dithiolate (after Ref. 103).

potential of the ring which reaches *ca* 1 V for a tetracyano derivative of porphyrin. The molecular area of the dicyano copper porphyrins **XII** and **XIII** were larger (2.20 nm²) than those of the dichained products **XIV** and **XV** which have an area of 0.89 and 1.10 nm², respectively. In these molecules, the porphyrin systems were vertically oriented. Copper cyanoporphyrin having four C₂₀H₄₁ groups forms better-quality films. The conductivities measured for compound **XII** were 10^{−6} S cm^{−1} in air and 10^{−1} S cm^{−1} under iodine pressure of 0.8 mm Hg.

3.2.3 Metal(4,5-dimercapto-1,3-dithiol-2-dithiolene)₂ complexes

Watanabe *et al.*¹⁰³ reported LB films of long alkylammonium dithiolate nickel complexes; C₁₈-Ni(pdt)₂, C₁₈-Ni(tdt)₂, and C₁₈-Ni(mnt)₂ (Fig. 20). The room-temperature conductivities of stam/C₁₈-Ni(pdt)₂, measured as a function of the number of the layer (*N* = 1–21), were in the range of 10^{−15}–10^{−16} S cm^{−1}. The in-perpendicular conductivities for 11 layers of stam/C₁₈-Ni(pdt)₂ were 10^{−17} S cm^{−1} at −120 °C and 10^{−14} S cm^{−1} at approx. 30 °C. On the other hand, in-parallel conductivities for 11 layers of stam/C₁₈-Ni(pdt)₂ were 10^{−4} S cm^{−1} at −120 °C and 10^{−2} S cm^{−1} at approx. 30 °C.

Mixed-valence complexes of metal(dmit)₂ complexes, where dmit stands for 4,5-dimercapto-1,3-dithiol-2-dithine, are an important class of conducting organic materials. TTF[Ni(dmit)₂]₂ at 1.6 K at 7 kbar,¹⁰⁴ α'-TTF-[Pd(dmit)₂]₂ at 6.42 K at 20.7 kbar,¹⁰⁴ and Me₄N[Ni(dmit)₂]₂ at 5 K at 7 kbar¹⁰⁵ (where TTF = tetrathiafulvalene and Me = methyl) are three molecular superconductors formed from the sulfur-rich 1,2-dithiolene complexes. Nakamura *et al.*^{58, 106, 107} prepared conducting LB films based on ammonium metal(dmit)₂ where monoalkyl- to tetraalkyl-

substituted ammonium were used as the counteranions (Fig. 21). The monolayers of the 1:1 mixture with icosanoic acid were transferred onto a solid substrate by a horizontal lifting method, except for 2C₁₆-Ni(dmit)₂, 2C₁₈-Ni(dmit)₂, and 2C₂₂-Ni(dmit)₂ where a vertical dipping method was used. Electrical conductivities of the LB films of metal(dmit)₂ complexes are listed in Table 6. The following is the essence of the conductivity results:

- (1) Most LB films showed conductivity in the range 0.1–1 S cm^{−1} and conductivity was larger for short alkyl-chain complexes.
- (2) Conductivities of dialkyldimethylammonium [2C_{*n*}-Ni(dmit)₂] and trialkylammonium [3C_{*n*}-Ni(dmit)₂] nickel(dmit)₂ complexes were in the same range.
- (3) The LB films of 3C_{*n*}-Au(dmit)₂ showed the largest conductivities, reaching 19 and 33 S cm^{−1} for 3C₁₀-Au(dmit)₂ and 3C₁₄-Au(dmit)₂ after electrochemical oxidation, respectively. The LB films of tridecylmethylammoniumAu(dmit)₂ [3C₁₀-Au(dmit)₂] exhibited metallic behavior down to *ca* 200 K, with a weak temperature dependence.

The preparation of LB films of a new Ni(dmit)₂ charge-transfer complex, (*N*-octadecylpyridinium)₂-Ni(dmit)₂ with *o*-hexadecylthiocarboxytetrathiafulvalene (HDTTTF) (Fig. 22) was described by Dhindsa *et al.*¹⁰⁸ Y-type LB films of the complex from a chloroform solution were deposited onto hydrophilic glass substrates at a pressure of 25–30 mN m^{−1}. The undoped complex has an electrical conductivity of 6 × 10^{−6} S cm^{−1} which increases to 0.8 S cm^{−1} upon doping with iodine. The conductivity data in the temperature range 300–100 K demonstrated space charge injection in both undoped and iodine-doped films. Alternate monolayers of the (*N*-octadecylpyridinium)₂-Ni(dmit)₂ complex with HDTTTF were also deposited onto a hydrophilic glass substrate from a chloroform solution. A 19-monolayer sample with ten layers of nickel complex and nine layers of HDTTTF showed a conductivity of 1 × 10^{−6} S cm^{−1}. Doping with iodine raised the con-

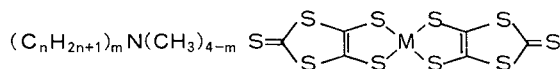


Figure 21 Structure of metal(4,5-dimercapto-1,3-dithiol-2-dithione) complexes, mC_{*n*}-M(dmit)₂ (after Refs 58, 106, 107).

Table 6 Electrical conductivities of the LB films of metal(dmit)₂ complexes (after Refs 58, 106). (Reprinted with permission from Plenum Press, after ref. 107, Nakamura, T *et al.*)

Material Cn-M(dmit) ₂ ^a	Conductivity (S cm ⁻¹)	
	Bromine oxidation	Electrochemical oxidation
1C ₁₈ -Ni(dmit) ₂	0.11	0.9
2C ₁₀ -Ni(dmit) ₂	1.0	1.4
2C ₁₂ -Ni(dmit) ₂	0.03	
2C ₁₄ -Ni(dmit) ₂	0.09	
2C ₁₆ -Ni(dmit) ₂	0.05	
2C ₁₈ -Ni(dmit) ₂	0.009	
2C ₂₂ -Ni(dmit) ₂ ^{b,c}	0.002	
3C ₁₀ -Ni(dmit) ₂	1.5	1.4
3C ₁₄ -Ni(dmit) ₂	1.3	0.87
4C ₁₀ -Ni(dmit) ₂	1.6	0.012
C ₁₄ Py-Ni(dmit) ₂ ^d	1.51	1.2
C ₂₂ Py-Ni(dmit) ₂	0.23	0.32
2C ₁₀ -Au(dmit) ₂	0.12	1.4
2C ₁₄ -Au(dmit) ₂	0.15	
2C ₁₈ -Au(dmit) ₂	0.005	
2C ₂₂ -Au(dmit) ₂	Undetectable	
3C ₁₀ -Au(dmit) ₂	15	33
3C ₁₄ -Au(dmit) ₂	5.4	19
3C ₁₆ -Au(dmit) ₂	2.6	0.46
3C ₁₈ -Au(dmit) ₂	1.4	0.12
(3C ₁₀) ₂ -Pd(dmit) ₂ ^b	0.3 (iodine doping ^c)	1.0
(2C ₁₀) ₂ -Pt(dmit) ₂ ^b	0.001 (iodine doping ^c)	

^aThe molar mixing ratio with icosanoic acid was 1:1, except where indicated. LB films were prepared by the horizontal lifting method except where indicated. ^bUsed as pure materials. ^cA vertical dipping method was used to prepare this compound. ^dPy = pyridinium. ^eOxidized with iodine vapors.

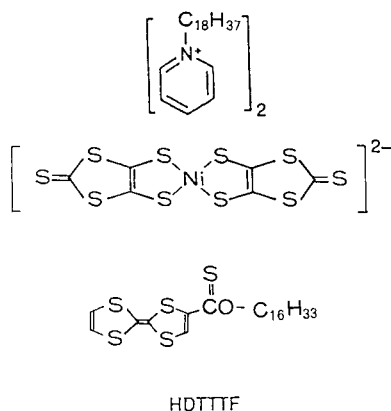


Figure 22 Chemical structure of (N-octadecylpyridinium)₂-Ni(dmit)₂ and o-hexadecylthiocarboxytetrathiafulvalene (HDTTF) (after Ref. 108).

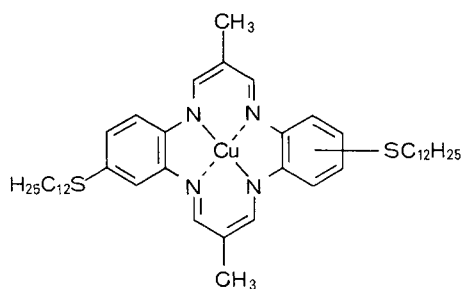


Figure 23 Bisdodecylthio-substituted copper dibenzotetra-aza[14]annulene (after Ref. 110).

ductivity to a maximum value of 0.1 S cm⁻¹. The LB films were characterized by transmission IR and X-ray photoelectron spectroscopy (XPS) techniques.

3.2.4 Metal(dibenzotetra-aza[14]annulene)s

The π -conjugated system of dibenzotetra-aza[14]annulenes shows high electrical conductivity upon doping with iodine.¹⁰⁹ Wegmann *et al.*¹¹⁰ synthesized a series of didodecylthio-substituted copper dibenzotetra-aza[14]annulenes (Fig. 23) from 4-dodecylthio-1,2-phenylenediamine, 3-ethoxy-2-methylacrylaldehyde and copper(II) acetate in dimethylformamide at 120 °C. LB monolayers of pure compounds could be transferred onto hydrophobic substrates. The deposition of monolayers from a mixture of methyl arachidate was more convenient. More than 50 layers can be deposited in a Y-type LB mode. The LB films (30 layers) of pure copper complex have an in-plane conductivity of 7.4×10^{-6} S cm⁻¹, which increases to 5.3×10^{-4} S cm⁻¹ upon iodine doping. The conductivity of a 2.3:1 mixture of complex and methyl arachidate in an undoped state was 6.7×10^{-6} S cm⁻¹ which increases by two orders of magnitude upon doping with iodine and aqueous potassium tri-iodide (KI₃) solution to 2.7×10^{-4} and 1.1×10^{-4} S cm⁻¹, respectively. The conductivity of LB films doped with potassium tri-iodide solution was found to be more stable than that of iodine-doped samples. Tieke and Wegmann¹¹¹ also reported another nickel complex of dibenzotetra-aza[14]annulene having four tetradecyloxy chains attached to the benzene ring and two pentadecyl chains (Fig. 24). LB films (30 layers) of a nickel complex deposited from a mixture with 80 mol % of cadmium arachidate show in-plane conductivity of 2.0×10^{-7} S cm⁻¹. Exposure to iodine vapor raised the conductivity to 4.0×10^{-6} S cm⁻¹.

3.2.5 Ferrocene derivatives

Ferrocene, which has multiple metal-to-carbon bonds, is one of the more interesting organometallic molecules used to prepare LB films. Electrochemically active LB films of polynuclear organometallic complexes comprising a diacetylene segment having metallocenes on both ends have also been prepared.¹¹² These organometallic complexes are photopolymerizable. LB films of 1,6-bis(stearoxyloxy)biferrocene in which the cyclopentadienyl rings of the ferrocene nucleus were oriented perpendicular to the films surface gave a mixed-valence monocation complex on oxidation.¹¹³

LB films of *N*-*n*-octadecylferrocene carboxamide (XVI), ferrocenyl-*n*-octadecanoate (XVII) and 1,1'-ferrocenylene dioctadecanoate (XVIII) have been described.¹¹⁴ These ferrocene derivatives (Fig. 25) have one or two long alkyl chains with a hydrophilic amide or ester linkage. The ferrocene derivative, XVI showed a dielectric constant of approx. 2.93. High electrical conductivity was anticipated for the LB films of the ferrocene amide derivative which has an ionization potential of 511 kJ mol⁻¹. LB films of the long-chain derivatives of ferrocene and biferrocene and oxidized ferricenium were also prepared.¹¹⁵ The ferrocene derivatives with one long chain showed a limiting area of 0.26 nm² molecule⁻¹ for ferrocene amide and 0.23 nm² molecule⁻¹ for the ester. The areas for the ferrocene and biferrocene with two alkyl chains were 0.45–0.46 nm² molecule⁻¹. Charge-transfer complexes of ferrocene and biferrocene derivatives with electron acceptors such as iodine, TCNQ and tetrafluoroborate were also examined. A 1:1 complex of TCNQ and a ferrocene derivative, both containing a long alkyl chain, formed a stable condensed monolayer. The isotherm characteristics of the complex were different from the parent amphiphiles. Likewise, iodine and tetrafluoroborate complexes also formed stable monolayers. The electrochemical oxidation and reduction in LB films of ferrocene

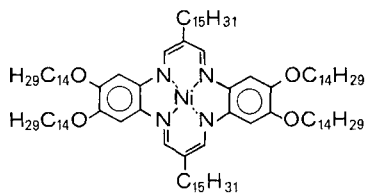


Figure 24 Nickel dibenzotetra-aza[14]annulene with tetradecyloxy groups (after Ref. 111).

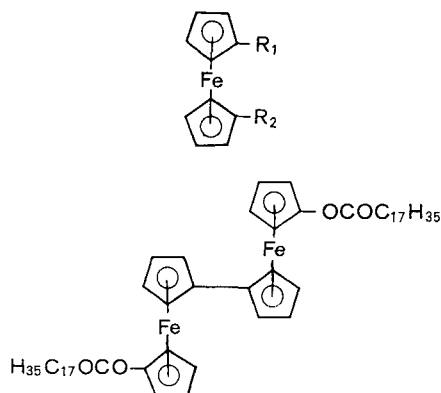


Figure 25 (a) Chemical structure of *N*-*n*-octadecylferrocene carboxamide (XVI), ferrocenyl-*n*-octadecanoate (XVII) and 1,1'-ferrocenylene dioctadecanoate (XVIII) (after Ref. 114). XVI: R₁ = CONHC₁₈H₃₇, R₂ = H; XVII: R₁ = OCOC₁₇H₃₅, R₂ = H; XVIII: R₁ = OCOC₁₇H₃₅ = R₂. (b) Biferrocene derivative (after Ref. 115).

derivatives on an ITO electrode were examined. Facci *et al.*¹¹⁶ prepared monolayer films of (ferrocenylmethyl) dimethyloctadecylammonium hexaphosphate (Fig. 26). The monolayer was spread from 50:50 vol % chloroform/benzene solutions. The limiting area was 0.51 nm² molecule⁻¹ on 0.1 mol dm⁻³ sodium sulfate, close to that calculated from molecular models (0.49 nm²). An amphiphilic terminally substituted conjugated nonaene with an end-group ferrocene has also been prepared.¹¹⁷ The molecular area of the polyenic acid containing ferrocene was estimated to be 0.42 nm² molecule⁻¹.

4 Organometallic LB films for nonlinear optics

The fundamental concepts of nonlinear optics and their relationship to chemical structures are well established,^{118,119} and are briefly summarized here in reference to second-order and third-order nonlinear optical effects. The microscopic polarization induced in an atom or a molecule by the appli-

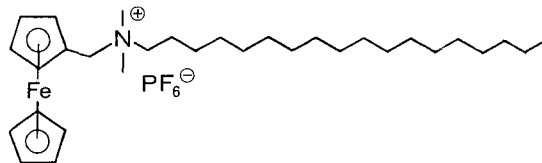


Figure 26 Chemical structure of (ferrocenylmethyl)-dimethyloctadecylammonium hexaphosphate (after Ref. 116).

Table 7 Nonlinear optical processes related to the input and output frequencies for measuring second-order and third-order nonlinear susceptibilities^{119, 135}

Input frequency	Output frequency	Susceptibilities $\chi^{(n)}$	Nonlinear optical processes
Second-order nonlinear optical effects			
ω_1, ω_2	ω_3	$\chi_{ijk}^{(2)}(-\omega_3; \omega_1, \omega_2)$	Sum frequency generation
ω	2ω	$\chi_{ijk}^{(2)}(-2\omega; \omega, \omega)$	Second-harmonic generation (SHG)
$\omega, 0$	ω	$\chi_{ijk}^{(2)}(-\omega; \omega, 0)$	Pockel's effect
ω_1	ω_2, ω_3	$\chi_{ijk}^{(2)}(-\omega_1; \omega_2, \omega_3)$	Three-wave difference frequency generation
ω	0	$\chi_{ijk}^{(2)}(0; -\omega, \omega)$	Optical rectification
Third-order nonlinear optical effects			
$\omega_1, \omega_2, \omega_3$	ω_4	$\chi_{ijkl}^{(3)}(-\omega_4; \omega_1, \omega_2, \omega_3)$	Four-wave sum frequency mixing
ω	3ω	$\chi_{ijk}^{(3)}(-3\omega; \omega, \omega, \omega)$	Third-harmonic generation (THG)
ω_1, ω_2	ω_3, ω_4	$\chi_{ijkl}^{(3)}(-\omega_3; -\omega_4, \omega_1, \omega_2)$	Four-wave difference frequency mixing (four-wave parametric mixing, amplification oscillation)
ω	ω	$\chi_{ijk}^{(3)}(-\omega; -\omega, \omega, \omega)$	Degenerate four-wave mixing, optical field induced birefringence, self-focusing, optical Kerr effect
$\omega, 0$	ω	$\chi_{ijk}^{(3)}(-\omega; 0, 0, \omega)$	DC Kerr effect
$\omega, 0$	2ω	$\chi_{ijk}^{(3)}(-2\omega; 0, \omega, \omega)$	Electric field induced second-harmonic generation (EFISH)
ω_1	ω_2	$\chi_{ijk}^{(3)}(-\omega_2; -\omega_1, \omega_1, \omega_2)$	Stimulated Raman, Brillouin and electronic Raman scattering
ω	ω	$\chi_{ijk}^{(3)}(-\omega; \omega, \omega, \omega)$	Degenerated two-photon absorption

cation of an external electrical field E can be described by Eqn [3]:

$$P_i = \alpha_{ij}E_j + \beta_{ijk}E_jE_k + \gamma_{ijkl}E_jE_kE_l + \dots \quad [3]$$

where P and E are related to the tensor quantities α , β , and γ referred to as the polarizability, second-order hyperpolarizability and third-order hyperpolarizability, respectively. Here, β and γ are associated with the second- and third-order nonlinear optical responses of molecules. Likewise, the macroscopic polarization induced in bulk media can also be expanded in the external field power series (Eqn [4]):

$$P_i = P_0 + \epsilon_0(\chi_{ij}^{(1)}E_j + g_1\chi_{ijk}^{(2)}E_jE_k + g_3\chi_{ijkl}^{(3)}E_jE_kE_l + \dots) \quad [4]$$

where $\chi^{(n)}$ are tensor quantities, and g_1 and g_3 are degeneracy factors arising from the intrinsic permutation symmetry; $\chi^{(1)}$, $\chi^{(2)}$ and $\chi^{(3)}$ have similar meanings to their microscopic counterparts α , β , and γ respectively. In these formulations, the even tensor $\chi^{(2)}$ is zero in centrosymmetric media, whereas the odd tensor $\chi^{(3)}$ does not have any symmetry restrictions. By knowing the magnitude of microscopic counterparts, a general trend of the corresponding macroscopic coefficients can be estimated. Table 7 lists nonlinear optical processes related to the input and

output frequencies for measuring second-order and third-order nonlinear susceptibilities. Optical phenomena such as second-harmonic generation, linear electro-optic effects or Pockels effects, parametric oscillation, rectification, etc., arise from $\chi^{(2)}$; and the Kerr effect, third-harmonic generation and Raman, Brillouin and Rayleigh scatterings arise from $\chi^{(3)}$. The $\chi^{(2)}$ and $\chi^{(3)}$ susceptibilities are related to molecular hyperpolarizabilities α , β and γ by Eqns [5]–[7]:

$$\chi^{(1)}(-\omega; \omega) = N\alpha F(\omega)F(\omega) \quad [5]$$

$$\chi^{(2)}(-2\omega; \omega, \omega) = 2N\beta F(2\omega)F(\omega)F(\omega) = 2d \quad [6]$$

$$\chi^{(3)}(-3\omega; \omega, \omega, \omega) = 4N\gamma F(3\omega)F(\omega)F(\omega)F(\omega) = 4C \quad [7]$$

where N is the density and $F(\omega)$ is the local field factor at frequency ω ; d and C are the second-order and third-order nonlinear coefficients. Large second-order optical nonlinearity originates from organic conjugated molecules having an electron-acceptor group at one end and a donor group at the opposite end. The acceptor and donor groups that are generally attached to conjugated systems such as benzene, azobenzene, stilbene, tolans and benzyldene are:

- (1) Acceptor groups: NO_2 , CN , COOH , CONH_2 , CHO , SO_2R , COCH_3 , SO_2NH_2 , and NH_3^+ .

- (2) Donor groups: NH_2 , NHR , NR_2 , F , Cl , Br , CH_3 , OH , NHCOCH_3 , OCH_3 , O^- and S^- .

A variety of organic materials having electron-acceptor and donor groups have been synthesized particularly for second-harmonic generation. The donor-acceptor substituted molecules can be utilized for third-order nonlinear optics (NLO). Figure 27 shows that NLO-active molecules could be designed, based on the principle that applies to amphiphiles by varying chemical structures that generate NLO effects. The NLO-active LB molecule has an electron-acceptor group at one end and a donor group containing a hydrophobic tail at the opposite end of a polarizable π -electron conjugated system. These amphiphilic dyes are suitable LB molecules for second-order nonlinear optics. The proper combination of strong donor-acceptor groups and a large conjugated region usually gives rise to relatively high second-order optical nonlinearity. Table 8 lists second-order nonlinear optical properties of organic LB materials.¹²¹⁻¹²⁷ Details of LB techniques and second-order NLO properties of heterotype LB films have recently been reviewed by Tieke,⁵⁹ Nalwa *et al.*,¹¹⁹ Okada and Nakanishi.¹²⁸ Organic LB films show second-order optical nonlinearity as high as 10^{-6} esu or even higher.

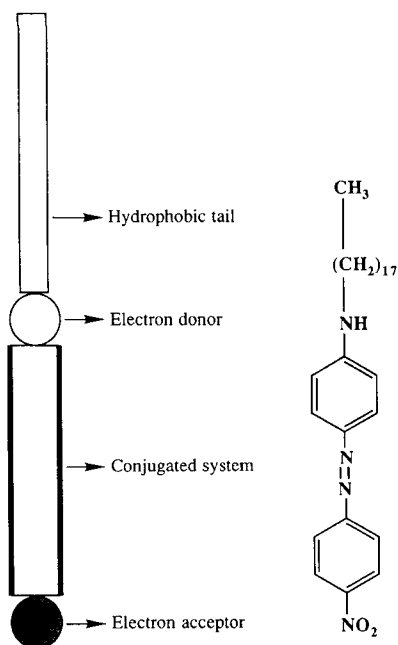


Figure 27 Structure of an NLO-active amphiphile with example.

4.1 Second-order nonlinear optical effects in organometallic LB films

Specialized aspects of second-order nonlinear optics have recently been summarized in a monograph presenting current knowledge of measurement techniques for organic molecular and polymeric materials.¹¹⁹ Organometallic materials are attractive in the field of nonlinear optics owing to the fact that charge-transfer interactions between metals and ligands may play a major role. Organometallics which crystallize in noncentrosymmetric space groups are interesting materials for second-order nonlinear optics. Large molecular hyperpolarizability arises in organometallic materials due to the transfer of electron density between the metal atoms and the conjugated ligand systems. In addition, the availability of metal atoms, and their incorporation with a variety of conjugated ligands, make them versatile materials for nonlinear optics. The first comprehensive description of organometallic NLO materials was published in this Journal by one of the present authors¹²⁹ and covered a wide variety of organometallic materials such as ferrocene derivatives, metal carbonyl complexes, metal-pyridine and bipyridine complexes, metal dithiolenes, organometallic thiourea complexes, metal acetylides, poly(metalynes), metallophthalocyanines, metalloporphyrins, metallocenes, polysilanes and organometallic charge-transfer complexes.

Organometallic materials are a new class of NLO materials and novel materials are still emerging. Recently, Wright *et al.*¹³⁰ reported second-harmonic generation from an organometallic polymer having pendant ferrocene chromophores in a poly(methyl methacrylate) copolymer. The corona-poled organometallic polymer showed a nonlinear d coefficient of 1.72 pmV^{-1} , which is about four times that of the quartz standard. In this review, we describe organometallic materials that form LB films to be utilized for studying second-order and third-order nonlinear optical interactions.

4.1.1 Organoruthenium complexes

Organoruthenium complexes have not only attracted attention for large pyroelectric coefficients but for second-harmonic generation also. Richardson *et al.*¹³¹ described LB films of a series of organoruthenium complexes having a ruthenium(cyclopentadienyl) bis(triphenylphosphine) head-group. The chemical structures of these complexes are shown in Fig. 28. The alkoxy chain

Table 8 Organic LB molecules for second-harmonic generation

Chemical structure ^a	$\chi^{(2)}$ (pm V ⁻¹)	Ref.
1		
2		
Alternating layers of 1 and 2	5.4 ± 0.8	121
3		
4		
Alternating layers of 3 and 4	340	121
5	13.6	122
6	17.6	123
7	30	124
8	43	124
9	64	124
10	14	124
11	25	124
12	76	124
13	146	124
14	36	124
15	15	124
16		
17		
Alternating layers of 16 and 17	840	125
18	7.6	27
19	16	126
20	$\beta = 51 \times 10^{-50} (\text{C}^3 \text{m}^3 \text{J}^{-2})$	127
21	$\beta = 46 \times 10^{-50} (\text{C}^3 \text{m}^3 \text{J}^{-2})$	127
22	$\beta = 85 \times 10^{-50} (\text{C}^3 \text{m}^2 \text{J}^{-2})$	127

- 1 $\text{CH}_3-(\text{CH}_2)_{17}-\text{N}(\text{CH}_3)-\text{C}_6\text{H}_4-\text{COOH}$
NO₂
- 2 $\text{CH}_3-(\text{CH}_2)_{16}-\text{OOC}-\text{C}_6\text{H}_4-\text{NH}-(\text{CH}_2)_2-\text{COOH}$
- 3 $\text{CH}_3-(\text{CH}_2)_{11}-\text{N}(\text{CH}_3)-\text{C}_6\text{H}_4-\text{N}=\text{N}-\text{C}_6\text{H}_4-\text{COOH}$
NO₂
- 4 $\text{HOOC}-(\text{CH}_2)_2-\text{N}(\text{CH}_3)-\text{C}_6\text{H}_4-\text{N}=\text{N}-\text{C}_6\text{H}_4-\text{COO}-(\text{CH}_2)_{16}-\text{CH}_3$
NO₂
- 5 $\text{CH}_3-(\text{CH}_2)_{21}-\text{NH}-\text{C}_6\text{H}_4-\text{NO}_2$
- 6 $\text{CH}_3-(\text{CH}_2)_{17}-\text{NH}-\text{C}_6\text{H}_4-\text{N}=\text{N}-\text{C}_6\text{H}_4-\text{NO}_2$
- 7 $\text{CH}_3-(\text{CH}_2)_{15}-\text{O}-\text{C}_6\text{H}_4-\text{CH}=\text{N}-\text{NH}-\text{C}_6\text{H}_4-\text{NO}_2$
- 8 $\text{CH}_3-(\text{CH}_2)_{17}-\text{O}-\text{C}_6\text{H}_4-\text{CH}=\text{N}-\text{NH}-\text{C}_6\text{H}_4-\text{NO}_2$
OH
- 9 $\text{CH}_3-(\text{CH}_2)_{17}-\text{S}-\text{C}_6\text{H}_4-\text{CH}=\text{N}-\text{NH}-\text{C}_6\text{H}_4-\text{NO}_2$
- 10 $\text{CH}_3-(\text{CH}_2)_{15}-\text{O}-\text{C}_6\text{H}_4-\text{CH}=\text{N}-\text{NH}-\text{C}_6\text{H}_4-\text{NO}_2$
NO₂
- 11 $\text{CH}_3-(\text{CH}_2)_{15}-\text{O}-\text{C}_6\text{H}_4-\text{CH}=\text{CH}-\text{CH}=\text{N}-\text{NH}-\text{C}_6\text{H}_3(\text{NO}_2)_2$
- 12 $\text{CH}_3-(\text{CH}_2)_{17}-\text{S}-\text{C}_6\text{H}_4-\text{CH}=\text{CH}-\text{C}_6\text{H}_4\text{N}^+\text{CH}_3$
I⁻
- 13 $\text{CH}_3-(\text{CH}_2)_{15}-\text{N}(\text{CH}_3)-\text{C}_6\text{H}_4-\text{CH}=\text{CH}-\text{C}_6\text{H}_4\text{N}^+\text{CH}_3$
I⁻
- 14 $\text{CH}_3-(\text{CH}_2)_{17}-\text{O}-\text{C}_6\text{H}_4-\text{CH}=\text{CH}-\text{C}_6\text{H}_4\text{N}^+\text{CH}_3$
I⁻
- 15 $\text{CH}_3-(\text{CH}_2)_{15}-\text{O}-\text{C}_6\text{H}_3(\text{OCH}_2)_2-\text{CH}=\text{N}-\text{NH}-\text{C}_6\text{H}_4-\text{NO}_2$
CH₃-(CH₂)₁₅-O
- 16 $\text{HOOC}-(\text{CH}_2)_2-\text{N}(\text{CH}_3)-\text{C}_6\text{H}_4-\text{CH}=\text{CH}-\text{CH}=\text{CH}-\text{CH}=\text{CH}-\text{CH}=\text{CH}-\text{CH}=\text{CH}-\text{COO}-(\text{CH}_2)_{11}-\text{CH}_3$
CN
- 17 $\text{CH}_3-(\text{CH}_2)_{11}-\text{N}(\text{CH}_3)-\text{C}_6\text{H}_4-\text{CH}=\text{CH}-\text{CH}=\text{CH}-\text{CH}=\text{CH}-\text{CH}=\text{CH}-\text{CH}=\text{CH}-\text{COOH}$
CN
- 18 $\text{CH}_3-(\text{CH}_2)_{17}-\text{NH}-\text{C}_6\text{H}_3(\text{NO}_2)_2$
- 19 $\text{CH}_3-(\text{CH}_2)_{17}-\text{NH}-\text{C}_6\text{H}_3(\text{NO}_2)_2$
F
- 20 $\text{C}_6\text{H}_4(\text{CH}_3)_2-\text{CH}=\text{CH}-\text{CH}=\text{CH}-\text{CH}=\text{CH}-\text{CH}=\text{CH}-\text{CH}=\text{CH}-\text{CHO}$
- 21 $\text{C}_6\text{H}_4(\text{CH}_3)_2-\text{CH}=\text{CH}-\text{CH}=\text{CH}-\text{CH}=\text{CH}-\text{CH}=\text{CH}-\text{CH}=\text{CH}-\text{CH}=\text{CH}-\text{N}(\text{CH}_2\text{CH}_2\text{CH}_2\text{CH}_3)_2$
- 22 $\text{C}_6\text{H}_4(\text{CH}_3)_2-\text{CH}=\text{CH}-\text{CH}=\text{CH}-\text{CH}=\text{CH}-\text{CH}=\text{CH}-\text{CH}=\text{CH}-\text{CH}=\text{CH}-\text{N}^+(\text{CH}_2\text{CH}_2\text{CH}_2\text{CH}_3)_2$
H C₁₈H₃₇

molecular hyperpolarizability in the range of $10\text{--}50\text{ C}^3\text{ m}^3\text{ J}^{-2}$ and good chemical stability.¹³²

Sakaguchi *et al.*¹³³ reported second-harmonic light emission from LB films of a ruthenium (II)–pyridine complex (Fig. 29). Alternate LB films of a matrix layer of $2\text{C}_{18}\text{NB}$ and a dye layer of RuC_{18}B and $2\text{C}_{18}\text{NB}$ in a 1:4 molar ratio were deposited. The second-harmonic light intensity from RuC_{18}B – $2\text{C}_{18}\text{NB}$ LB films decreased to ca 50% when the complex was irradiated by other laser pulses at either 355 nm or 460 nm just before Nd:YAG laser irradiation at 1064 nm. The LB films prepared from 1-methyl-4-[4-octadecyl-*N*-methylamino]styryl]–pyridinium iodide (C_{18}AStZ) and C_{18}NB in a 2:3 molar ratio showed strong second-harmonic generation and, in this case, the second-harmonic light intensity was not affected by irradiation by dye laser pulses, unlike RuCl_{18}C – $2\text{C}_{18}\text{NB}$ LB films where second-harmonic intensity was reduced to 50% of that without UV-laser irradiation. This change in molecular hyperpolarizability has been considered to be associated with a ground state metal-to-ligand charge-transfer excited state. This phenomenon from RuC_{18}B – $2\text{C}_{18}\text{NB}$ LB films may have an application as an optical switch.

4.1.2 Siloxane polymers

Carr *et al.*¹³⁴ reported second-harmonic generation (SHG) in a monomolecular LB film of a polysiloxane consisting of poly(dimethylsilane) and poly(methylsilane) units of unspecified distri-

bution. The chemical structure of the corresponding polysiloxane is shown in Fig. 30.

This polysiloxane has a hydroxy group as a hydrophilic head-group to provide stability to the monolayer. The pendant chromophore contains a conjugated azobenzene group and an ether oxygen group. The polysiloxane backbone has only about 50 % of pendant chromophoric groups. A monolayer of the polymer was spread from a dichloromethane solution onto an aqueous sub-phase at pH 5.5 at 20 °C. From the isotherm, the average area per chromophoric side-group was estimated to be ca 0.38 nm^2 at $\pi = 30\text{ mN m}^{-1}$. For SHG measurements, an LB monolayer was deposited onto a hydrophilic glass substrate. The second-harmonic intensity from a monolayer was compared with hemicyanine which had a molecular hyperpolarizability β of $3.5 \times 10^{-49}\text{ C}^3\text{ m}^3\text{ J}^{-2}$, whereas the hyperpolarizability β of merocyanine was taken as $9 \times 10^{-49}\text{ C}^3\text{ m}^3\text{ J}^{-2}$, assuming that the refractive indices of both materials are the same.

4.2 Third-order nonlinear optical effects in organometallic LB films

Organic π -electron conjugated polymers have been considered as model systems for third-order nonlinear optical interactions because of their ultrafast response time, high optical nonlinearity and high laser damage thresholds. Third-order nonlinear optical properties of a very wide variety of organic materials such as dyes, π -conjugated polymers, charge-transfer complexes, NLO-chromophore grafted polymers, composites and organometallics have been investigated. A recent monograph¹³⁵ by the present authors gives a detailed description of third-order organic materials, measurement techniques for third-order optical nonlinearity and quantum chemistry approaches to calculate hyperpolarizability.

Interest in third-order nonlinear optical properties of conjugated polymers originated from the discovery by Sauteret *et al.*,¹³⁶ who demonstrated for the first time that the poly(diacetylene) polymer of 2,4-hexadiyn-1,6-diol bis(*p*-toluene sulfonate) PTS has a $\chi^{(3)}$ of $8.5 \times 10^{-10}\text{ esu}$. Polydiacetylenes can be processed into LB films. Their third-order NLO properties are discussed here. Carter *et al.*¹³⁷ reported a $\chi^{(3)}$ of ca $2.8 \times 10^{-11}\text{ esu}$ for poly(diacetylene) LB films in the 750–1050 nm range. Kajzar and Messier¹³⁸ conducted wave-dispersed third-harmonic generation measurements on LB films of poly(diacetylene) in

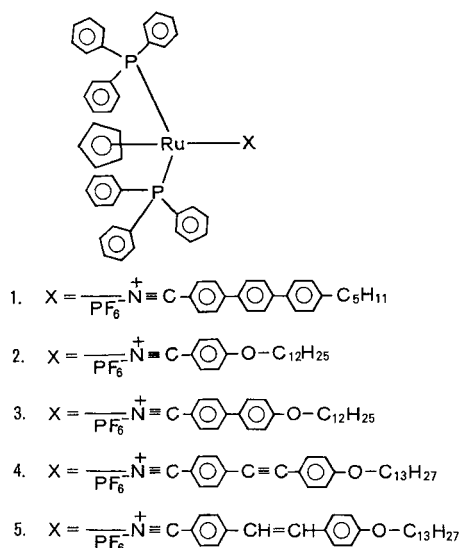
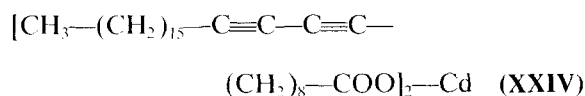


Figure 28 Organoruthenium complexes showing large second-order hyperpolarizability. 1 = XIX, 2 = XX, 3 = XXI, 4 = XXII, 5 = XXIII (after Ref. 131).

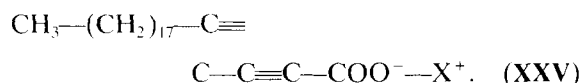
Table 9 Molecular hyperpolarizabilities of ruthenium complex LB films determined from electric field induced second-harmonic generation (EFISH) (after Ref. 131)

Ruthenium complex LB films	Absorption maximum, λ_{max} (nm)	Hyperpolarizability (β) (10^{-30} esu)
XX	247	3.5
XXI	292	20
XXII	327	25
XXIII	342	37

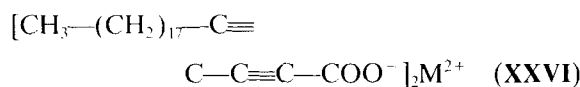
the 800–1900 nm wavelength region. Mono-molecular films of the diacetylene molecule **XXIV**



were transferred onto a silica substrate by the LB technique. The LB multilayers showed the existence of two resonances in $\chi^{(3)}$: first a two-photon resonance around 1350 nm and a three-photon resonance at 1097 nm. The resonant $\chi^{(3)}$ values were 1.5×10^{-10} esu at 1350 nm and 2.2×10^{-12} esu at 1097 nm. Kajzar and Messier¹³⁹ also reported the solid-state polymerization and NLO properties of diacetylene LB films of **XXV** and **XXVI**.



X = H, NH_4 , Ag, Na



M = Cd, Cu, Hg, Mn

The diacetylene monovalent salt of NH_4^+ and Ag^+ and the acid form polymerize, while Na^+ and the divalent salts do not polymerize. Third-harmonic generation measurements carried out with a

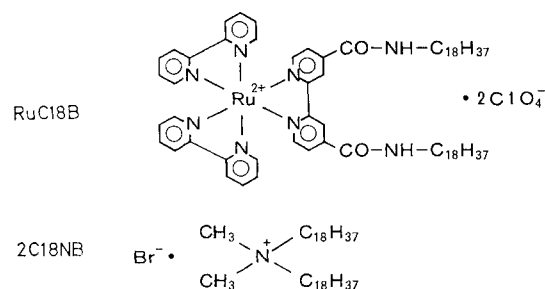
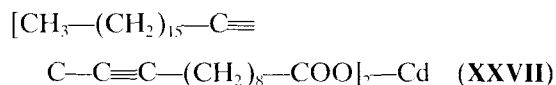


Figure 29 Organoruthenium(II)-pyridine complexes (after Ref. 133).

Q-switched Nd:YAG laser at the fundamental wavelength of 1064 nm gave a $\chi^{(3)}$ of 0.67×10^{-12} esu for the ammonium salt polymer. LB multilayers of a polymer with a diacetylene groups in the middle of the aliphatic chain, viz. **XXVII**,



showed a $\chi^{(3)}$ value of 0.69×10^{-12} esu under similar conditions. The nonlinear optical susceptibility of the most stable ammonium salt polymer was almost the same as that of a cadmium salt polymer. The electric field-induced-second-harmonic generation (EFISH) measurements for

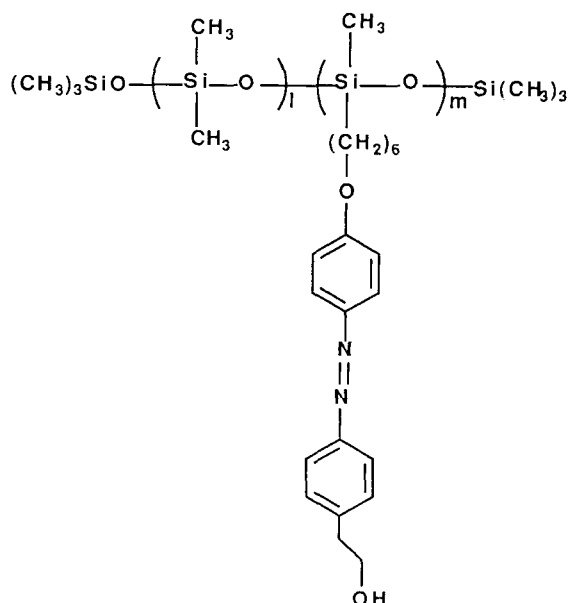
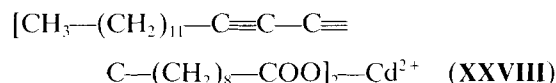


Figure 30 Chemical structure of a polysiloxane with pendant NLO chromophore ($P = 9 \pm 2$; $m = 8 \pm 2$). (After ref. 134.)

LB multilayers of **XXVIII** with a fundamental wavelength ranging from 800 to 1400 nm showed a $\chi^{(3)}$ maximum around 1350 nm.¹⁴⁰ Observation by crossed polarizers indicated that the LB layers seem to be made of single microcrystals oriented randomly around the normal to the substrate. Therefore the value of $\chi^{(3)}(-2\omega; \omega, \omega, 0)$ was an average for a single crystal over all orientations in the substrate plane. From Eqn [8]:

$$\chi^{(3)}(-2\omega; \omega, \omega, 0) = 1/\langle \cos^4\theta \rangle \chi^{(3)} \text{LB}(-2\omega; \omega, \omega, 0) \quad [8]$$

where $\langle \cos^4\theta \rangle = 3/8$, the value of $\chi^{(3)}$ at 1150 nm was 1.3×10^{-12} esu. This $\chi^{(3)}$ value was almost the same as the value of $\chi^{(3)} \text{LB}(-3\omega; \omega, \omega, \omega) = 1.33 \times 10^{-12}$ esu estimated by third harmonic generation (THG) measurements at 1064 nm.¹⁴¹ Poly(diacetylene) monovalent and divalent salts show interesting third-order nonlinear optical properties; the magnitude was within the range of that found for thin films. To the best of our knowledge, third-order NLO properties of organometallic LB films have never been studied so far.

4.2.1 Polysilanes

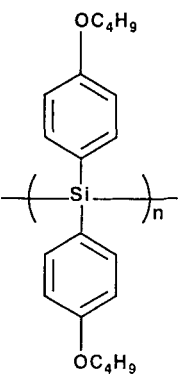
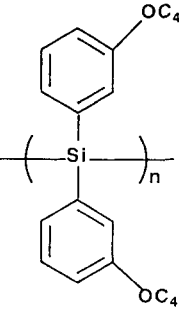
Polysilanes are an interesting class of electronic and photonic materials. In polysilanes, the delocalization of the σ -orbitals of the silicon-silicon (Si-Si) single bonds in the backbone plays a significant role. The optical transparency of silane polymers is of particular interest in the study of nonlinear optical interactions.

Kajzar *et al.*¹⁴² first reported third-order nonlinear optical properties of isotropic films of poly-(methylphenylsilane), which has a third-order optical susceptibility $\chi^{(3)}$ of 1.5×10^{-12} esu. This report stimulated further research on NLO properties of polysilanes and, as a result, polysilane backbone, containing different side-groups were investigated. Third-order nonlinear optical properties of a variety of substituted polysilanes have recently been summarized by the present authors in a monograph.¹³⁵

Of particular interest for this review are the third-order nonlinear optical properties of polysilane LB films. Embs *et al.*¹⁴³ reported the preparation of LB films of about 20 different polysilanes. Low-molecular weight polysilane monolayers were spread from n-hexane solution, while very high-molecular-weight polysilane monolayers were obtained at an air-water inter-

face from a chloroform solution. Polysilane backbones having bis(*p*-butoxyphenyl) and bis(*m*-butoxyphenyl) substituents were evaluated for third-order nonlinear optical effects. Table 10 lists the chemical structures, and real and imaginary part, of third-order optical susceptibilities of these polysilanes. The third-order optical susceptibility $\chi^{(3)}$ is higher with the polarization of the fundamental light parallel to the dipping direction than that of perpendicular polarization. The angular dependence of $\chi^{(3)}$ of the polybis(*m*-butoxyphenyl) polymer showed that $\chi^{(3)}$ is influenced by the oscillator strength of the polysilane backbone, rather than by phenyl-ring absorption. Annealing of the samples at elevated temperatures gave a strong increase in anisotropy and the largest absolute $\chi^{(3)}$ value of 4×10^{-12} esu was determined for an annealed sample. Poly bis(*m*-butoxyphenyl)silane showed the largest

Table 10 Third-order nonlinear optical susceptibilities of polysilane LB films. (after Ref. 143)

Polysilane	Re[$\chi^{(3)}$] 10 ⁻¹² esu	Im[$\chi^{(3)}$] 10 ⁻¹² esu	Orientation to the dipping direction
	0.9 0.5	0.3 0.1	Parallel Perpendicular
	(a) -2.7 -1.4 (b) -4.2 ^a -0.2 ^a	0.5 0.5 0.8 ^a 0.5 ^a	Parallel Perpendicular Parallel Perpendicular

^a Samples annealed at 120 °C for 1 h.

Re = real, Im = imaginary

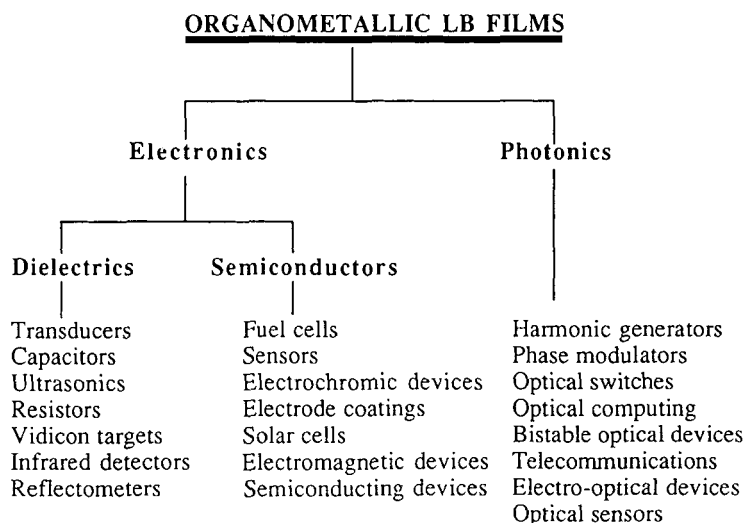


Figure 31 Possible application of organometallic LB films in electronics and photonics.

third-order susceptibility associated with the effective conjugated length along the polysilane backbone.

POSSIBLE APPLICATIONS

Applications of LB films may be considered in widespread areas of microelectronics and photonic technologies, particularly in those devices where a molecularly controlled thickness is required. Figure 31 shows the possible applications of organometallic LB films in electronic and photonic technologies. Polar dielectrics may have a very wide range of applications, ranging from solid-state technology to biomedical engineering, e.g. in detectors, vidicon targets, infrared sensors and transducers. Applications of organometallic LB films in infrared detectors,^{35–38} photovoltaic cells,⁷⁸ chemiresistors,⁸⁰ chemical sensors⁹³ and optical switches¹³³ have already been proposed. The fabrication of thin-film dielectrics from an amphiphilic two-ring phthalocyanine (OH)GePcOSiPc[Si(n—C₆H₁₃)₃], where Pc is the phthalocyanine dianion, has been suggested.¹⁴⁴ Monolayer and multilayers dielectrics may have potential in microelectronic devices. Polar dielectrics that lack a center of symmetry can exhibit second-order nonlinear optical responses; hence, they can be used as harmonic generators, electro-optical modulators, waveguides and other optoelectronic devices.^{135, 145} Extended π -conjugated materials are another class of nonlinear optical

materials since they show large third-order optical nonlinearities. Applications of these materials have been anticipated in optical communications, optical computing, optical signal processing and harmonic generators. Organometallic LB films can be used in energy conversion, chemical sensors, electroluminescences and electrochromic devices, electrocatalysis, field-effect transistors, microlithography, optical signal processing, modulators and harmonic generators.

6 CONCLUSIONS

This review has been the first attempt to survey literature on organometallic materials that form LB monolayers and multilayers. The literature survey conducted by using the *Chemical Abstracts* Service (CAS) from 1967 to 30 April 1992 showed only a few references on organometallic LB films. If we considered organometallic compounds having a metal-to-carbon bond, then the field of organometallic LB films remains almost unexplored. With this chemical aspect, the LB films of organoruthenium derivatives have been studied both for electrical and nonlinear optical properties. Ferrocene derivatives have been investigated from an electrochemical point of view. On the other hand, significant advances have been made on metal-containing phthalocyanines, porphyrins, (4,5-dimercapto-1,3-dithiol-2-dithionene)₂ complexes, and dibenzotetra-aza[14]annulenes where the metal atom is linked to nitrogen or sulfur

atoms. LB films of silicon-containing materials, where silicon is considered as a metaloidal element, are of particular interest because of their unique optical transparency and processability, but the magnitude of optical nonlinearity in polysilane LB films was found to be rather moderate. Looking at the electronic and photonic responses displayed by organometallic LB films, it becomes apparent that metal-to-ligand bonding plays an important role both in preparing LB films either with higher electrical conductivity as in metal(dmit)₂ complexes ($\sigma = 33 \text{ S}^{-1} \text{ cm}$) or with large optical nonlinearity as in organoruthenium complexes ($\beta = 50 \text{ C}^3 \text{ m}^3 \text{ J}^{-3}$). Even though some progress has been made, enormous opportunities exist to develop new organometallic LB materials and the challenge to design the novel organometallic molecules structurally to optimize the electrical and optical properties still remains. Further significant advances are expected in organometallic LB films with the evolution of novel robust materials with desired functions. Organometallic LB films seem promising for the future electronic and photonic technologies.

Acknowledgements The authors would like to thank Dr Shuji Okada of the Research Institute of Polymers and Textiles at Tsukuba for his generosity in providing articles of interest and for stimulating discussions and constructive suggestions.

REFERENCES

1. Walker, J R, Jr (ed.) *Chemistry and Physics of Carbon*, Marcel Dekker, New York, 1967
2. Weltner, W, Jr and Zee van J. *Chem. Rev.*, 1989, 89: 1713
3. Kroto, H W, Heath, J R, O'Brien, S C, Curl, R F and Smalley, R E *Nature*, 1985 (London), 318: 162
4. Kratschmer, W, Lamb, L D, Fostiropoulos, K and Haffman, D R, *Nature (London)*, 1990, 347: 354
5. Obeng, Y S and Bard, A J *J. Am. Chem. Soc.*, 1991, 113: 6279
6. Nakamura, T, Tachibana, H, Yumura, M, Matsumoto, M, Azumi, R, Tanaka, M and Kawabata, Y *Langmuir*, 1992, 8: 4
7. David, W I F, Ibberson, R M, Matthewman, J C, Prassides, K, Dennis, T J S, Hare, J P, Kroto, H W, Taylor, R and Walton, D R M *Nature (London)*, 1991, 147: 353
8. Holczer, K, Klein, O, Huang, S-M, Kaner, R B, Fu, K-J, Whetten, R L and Diederich, F *Science*, 1991, 252: 1154
9. Tanigaki, K, Ebbesen, T W, Saito, S, Mizuki, J, Tsai, J S, Kubo, Y and Kuroshima, S *Nature (London)*, 1991, 352: 222
10. Iqbal, Z, Baughman, R H, Ramakrishna, B L, Khare, S, Murthy, N S, Bornemann, H J and Morris, D E *Science*, 1991, 254: 826
11. Blau, W J, Bryne, H J, Cardin, D J, Dennis, T J, Hare, J P, Kroto, H W, Taylor, R and Walton, D R M *Phys. Rev. Lett.*, 1991, 67: 1423
12. Hoshi, H, Nakamura, N, Murayama, Y, Nakagawa, T, Suzuki, S, Shiromaru, H and Achiba, Y *Jpn. J. Appl. Phys.*, 1991, 30: 1397
13. Wang, X K, Zhang, T G, Lin, W P, Liu, S Z, Wong, G K, Kapper, M M, Chang, R P H and Ketserson, J B *Appl. Phys. Lett.*, 1992, 60: 810
14. Diederich, F and Whetten, R L *Acc. Chem. Res.*, 1992, 25: 119
15. So, H Y and Wilkin C L J. *Chem. Phys.*, 1989, 93: 1184
16. Kroto, H W, Allaf, A W and Balm, S P *Chem. Rev.*, 1991, 91: 1213
17. Hadden, R C *Acc. Chem. Res.*, 1992, 25: 134, and references therein
18. Nalwa, H S, *J. Macromol. Sci., Rev. Macromol. Chem. Phys.*, 1991, 31: 342
19. Franklin, B *Phil. Trans. Royal Soc.*, 1774, 64: 445
20. Pockels, A, *Nature (London)*, 1891, 43: 437; 1892, 46: 418; 1893, 48: 152; 1894, 50: 223
21. Rayleigh, L *Phil. Mag.*, 1899, 48: 321
22. Langmuir, I *J. Am. Chem. Soc.*, 1917, 39: 1848
23. Blodgett, K J. *Am. Chem. Soc.*, 1935, 57: 1007
24. Blodgett, K and Langmuir, I *Phys. Rev.*, 1937, 51: 964
25. Gaines, G *Insoluble Monolayers at Liquid-Gas Interfaces*, Interscience, New York, 1966
26. Nalwa, H S, Nakajima, K, Watanabe, T, Nakamura, K, Yamada, A and Miyata, S *Jpn. J. Appl. Phys.*, 1991, 30: 985
27. Lang, S B *Sourcebook of Pyroelectricity*, Gordon and Breach, New York, 1974
28. Agarwal, V K and Srivastava, V K *Thin Solid Films*, 1975, 27: 49
29. Kapur, U and Srivastava, V K *Phys. Status Solidi A*, 1976, 30: K77
30. Blinov, L M, Davydura, N N, Lazarev, V V and Yudin, S G *Sov. Phys. Solid State*, 1982, 24: 1523
31. Christie, P, Roberts, G G and Petty, M C *Appl. Phys. Lett.*, 1986, 48: 1101
32. Sakuhara, T, Nakahara, H and Fukuda, K *Thin Solid Films*, 1988, 159: 345
33. Novak, V R and Myagkov, I V *Prisma Zh. Tech. Fiz.*, 1985, 11: 385
34. Roberts, G G, Holcroft, B, Richardson, T and Colbrook, R J. *Chim. Phys.*, 1988, 85: 1093
35. Colbrook, R, Holcroft, B, Roberts, G G, Polywka, M E C and Davies, S G *Ferroelectrics*, 1989, 92: 381
36. Colbrook, R, Richardson, T, Roberts, G G, Smallridge, A and Davies, S G *Ferroelectrics*, 1991, 188: 209
37. Colbrook, R, Richardson, T, Poulter, M W, Roberts, G G, Polywka, M E C and Davies, S G *Mater. Sci. Eng.*, 1990, B7: 189

39. Daifuku, H, Aoki, K, Takuda, K and Matsuda, H *J. Electroanal. Chem.*, 1985, 183: 1
40. Miller, C J and Bard, A J *J. Electroanal. Chem.*, 1991, 63: 1707
41. Fujihira, M, Nishiyama, K and Aoki, K *Thin Solid Films*, 1988, 160: 317
43. Ferraris, J, Cowan, D O, Walatka, V, Jr and Perlstein, J H *J. Am. Chem. Soc.*, 1973, 95: 948
44. Jerome, D, Mazaud, A, Ribault, M and Bechgaard, K *J. Phys. (Paris)*, 1980, 41: L95
45. Saito, G and Kagoshima, S (eds) *The Physics and Chemistry of Organic Superconductors*, Springer-Verlag, Berlin, 1990
46. Ishiguro, T and Yamaji, K *Organic Superconductors*, Springer-Verlag, Heidelberg, 1990
47. Williams, J M *et al Organic Superconductors: Synthesis, Structure, Properties and Theory*, Prentice-Hall, New Jersey, 1991
48. Williams, J M, Schultz, A J, Geiser, U, Carlson, K D, Kini, A M, Wang, H H, Kwok, W K, Whangbo, M H and Schirber, J E *Science*, 1991, 252: 1501
49. Ivory, D M, Miller, G G, Sowa, J M, Shacklette, L W, Chance, R R and Baughman, R H *J. Chem. Phys.*, 1979, 71: 1506; Trivedi, D C, *J. Chem. Soc., Chem. Commun.*, 1990, 544
50. Nalwa, H S *J. Mater. Sci.*, 1992, 27: 210, and references therein
51. Nalwa, H S *Phys. Rev. B*, 1989, 39: 5964
52. Mott, N F *Phil. Mag.*, 1969, 19: 835
53. Su, W A, Schrieffer, J R and Heeger, A J *Phys. Rev. Lett.*, 1979, 42: 1698
54. Bredas, J L and Street, G B *Acc. Chem. Res.* 1985, 18: 309
55. Nalwa, H S *Appl. Organomet. Chem.*, 1990, 4: 91
56. Skotheim, T A (ed) *Handbook on Conducting Polymers*, vols 1 and 2, Marcel Dekker, New York, 1986
57. Techagumpuch, A, Nalwa, H S and Miyata, S Promising applications of conducting polymers. In: *Electroresponsive Organic Molecular and Polymeric Systems*, vol 2, Skotheim, T A (ed), Marcel Dekker, New York, 1991, chapter 5, pp 257-294
58. Nakamura, T and Kawabata, Y *Techno Japan*, 1989, 8: 22, and references therein
59. Tieke, B *Adv. Mater.*, 1990, 2: 222
60. Ferraro, J R and Williams, J M *Introduction to Synthetic Electrical Conductors*, Academic Press, Orlando, 1987
61. Ulman, A *Ultrathin Organic Films*, Academic Press, New York, 1991
62. Matsumoto, M, Nakamura, T, Manda, E, Kawabata, Y, Ikegami, K, Kuroda, S, Sugi, M and Saito, G *Thin Solid Films*, 1988, 160: 61
63. Saito, G *Pure Appl. Chem.*, 1987, 59: 999
64. Richard, J, Vandevyver, M, Barraud, A, Morand, J P, Lapouyade, R, Delhaes, P, Jacquinet, J F and Roullay, M, *J. Chem. Soc., Chem. Commun.*, 1988, 754
65. Kawabata, Y, Nakamura, T, Matsumoto, M, Tanaka, M, Sekiguchi, T, Komizu, H, Manda, E and Saito, G *Synth. Metals*, 1987, 19: 663
66. Dhindsa, A S, Bryce, M R, Lloyd, J P and Petty, M C *Thin Solid Films*, 1988, 165, L97
67. Bryce, M R, Dhindsa, A S and Petty, M C *ISSP Symposium on Organic Superconductors, Tokyo 1989*, Abstract No 13
68. Tieke, B and Wegmann, A *Thin Solid Films*, 1989, 179: 109
69. Raudel, A T, Vandevyver, M and Barraud, A *Mol. Cryst. Liq. Cryst.*, 1985, 120: 319
70. Nakamura, T, Matsumoto, M, Takei, F, Tanaka, M, Sekiguchi, T, Manda, E and Kawabata, Y *Chem. Lett.*, 1986, 709
71. Dhindsa, A S, Bryce, M R, Lloyd, J P and Petty, M C *Synth. Metals*, 1987, 22: 185
72. Sotnikov, P S, Berzina, T S, Troitsky, V I, Valter, R E, Karlivan, G A and Neiland, O Y *Thin Solid Films*, 1989, 179: 267
73. Hong, K and Rubner, M F *Thin Solid Films*, 1988, 160: 187
74. Watanabe, I, Hong, K, Rubner, M F and Loh, I H *Synth. Metals*, 1989, 28: C473
75. Ando, M, Watanabe, Y, Iyoda, T, Honda, K and Shimizu, T *Thin Solid Films*, 1989, 179: 225
76. Nishikata, Y, Kakimoto, M and Imai, Y, *J. Chem. Soc., Chem. Commun.*, 1988, 1040
77. Nichogi, K, Waragai, K, Taomoto, A, Saito, Y and Asakawa, S *Thin Solid Films*, 1989, 179: 297
78. Brynda, E, Koropeccky, I, Kalvoda, L and Nespurek, *Thin Solid Films*, 1991, 199: 375
79. Snow, A W, Barger, W R, Klusty, M, Wohltjen, H and Jarvis, N L *Langmuir*, 1986, 2: 513
80. Barger, W R, Snow, A W, Wohltjen, H and Jarvis, N L *Thin Solid Films*, 1985, 133: 197
81. Barger, W R, Wohltjen, H and Snow, A W *Transducers '85, Int. Conf. on Solid State Sensors and Actuators*, 1985, Dig. Tech. Pap. IEEE, New York, 1985, pp 410-413
82. Pace, M D, Barger, W R and Snow, A W *Langmuir*, 1989, 5: 973
83. Fujiki, M, Tabei, H and Imamura, S *Jpn. J. Appl. Phys.*, 1987, 26: 1224
84. Fujiki, M and Tabei, H *Langmuir*, 1988, 4: 320
85. Gupta, S K, Hann, R A and Twigg, M V *Thin Solid Films*, 1989, 179: 343
86. Hann, R A, Gupta, S K, Fryer, J R and Eyres, B L *Thin Solid Films*, 1985, 134: 35
87. Roberts, G G, Petty, M C, Baker, S, Fowler, M T and Thomas, N J *Thin Solid Films*, 1985, 132: 113
88. Ogawa, K, Kinoshita, S, Yonehara, H, Nakahara, H and Fukuda, K *J. Chem. Soc., Chem. Commun.*, 1989, 477
89. Palacin, S, Leareur, P, Stefanelli, I and Barraud, A *Thin Solid Films*, 1988, 159: 83
90. Kalina, D W and Crane, S W *Thin Solid Films*, 1985, 134: 109
91. Solinsh, E A, Mizikante, I J, Taure, L F and Shlihta, G A *J. Mol. Electr.*, 1991, 7: 127
92. Orthman, E and Wegner, G *Angew. Chem. Int. Ed.*,

- Engl., 1986, 25: 1105
93. Sauer, Th, Caser, W, Wegner, G, Vogel, A and Hoffmann, B J. *Phys. D, Appl. Phys.*, 1990, 23: 79
94. Ali-adib, Z, Davidson, K, Nooshin, H and Tredgold, R H *Thin Solid Films*, 1991, 201: 187
95. Petty, M, Lovett, D R, O'Connor, J M and Silver, J *Thin Solid Films*, 1989, 179: 387
96. Souto, J, Aroca, R and Desaja, J A J. *Raman Spectrosc.*, 1991, 22: 349
97. Clavijo, R E, Battisti, D, Aroca, R, Kovacs, G J and Jennings, C A *Langmuir*, 1992, 8: 113
98. Souto, J, Tomilova, L, Aroca, R and DeSaja, J A *Langmuir*, 1992, 8: 942
99. Tredgold, R H, Evans, S D, Hodge, P and Hoorfar, A *Thin Solid Films*, 1988, 160: 99
100. Mohwald, H, Miller, A, Stich, W, Knoll, W, Ruau-del-Teixier, A, Lehmann, T and Fuhrhop, J-H *Thin Solid Films*, 1986, 141: 261
101. Luk, S Y and Williams, J O J. *Chem. Soc., Chem. Commun.*, 1989, 158
102. McArdle, C B and Ruau-del-Teixier, A, *Thin Solid Films*, 1985, 133: 93
103. Watanabe, M, Kamiyama, H, Snaui, K and Ogata, N *Polym. Preprints Japan*, 1987, 36: 3242
104. Brossard, L, Ribault, M, Bousseau, M, Valade, L and Cassoux, P *Acad. Sci., Ser.* 1986, 302: 205; Brossard, L, Ribault, M, Valade, L and Cassoux, P J. *Phys. (Paris)*, 1987, 50: 1521
105. Kobayashi, A, Kim, H, Sasaki, Y, Kato, R, Kobayashi, H, Moriyama, S, Nishio, Y, Kajita, K and Sasaki, W *Chem. Lett.*, 1987, 1819
106. Nakamura, T, Tanaka, H, Kojima, K, Matsumoto, M, Tachibana, H, Tanaka, M and Kawabata, Y *Thin Solid Films*, 1989, 179: 183
107. Nakamura, T, Tachibana, H, Matsumoto, M, Tanaka, M and Kawabata, Y In: *Lower-Dimensional Systems and Molecular Electronics*, Metzger, R M (eds), Plenum Press, New York, 1991, and references therein
108. Dhindsa, A S, Badyal, J P, Pearson, C, Bryce, M R and Petty, M C J. *Chem. Soc., Chem. Commun.*, 1991, 322
109. Lin, L S, Marks, T J, Kannewurf, C R, Lyding, J W, McClure, M S, Ratajack, M T and Whang, T C J. *Chem. Commun.*, 1980, 954
110. Wegmann, A, Hunziker, M and Tieke, B J. *Chem. Soc., Chem. Commun.*, 1989, 1179
111. Tieke, B and Wegmann, A *Thin Solid Films*, 1989, 179: 109
112. Suzuno, J, Fukuda, A, Koyama, T, Hanabusa, K, Shirai, H and Nobumasa, H Japanese Patent JP 88-182395 (20 July 1988)
113. Sato, M, Nakahara, H, Fukuda, K and Akabori, S J. *Chem. Soc., Chem. Commun.*, 1988, 24
114. Nakahara, H, Fukuda, K and Sato, M *Thin Solid Films*, 1985, 133: 1
115. Nakahara, H, Katoh, T, Sato, M and Fukuda, K *Thin Solid Films*, 1988, 160: 153
116. Facci, J S, Falcigno, P A and Gold, J M *Langmuir*, 1986, 2: 732
117. Effenberger, F, Meller, P, Ringsdorf, H and Schlosser, H *Adv. Mater.*, 1991, 3: 555
118. Chemla, D S and Zyss, J (eds), *Nonlinear Optical Properties of Organic Molecules and Crystals*, vols 1 and 2, Academic Press, New York, 1987
119. Nalwa, H S, Watanabe, T, and Miyata, S, Optical second harmonic generation in organic molecular and polymeric materials: measurement techniques and materials. In: *Progress in Photochemistry and Photophysics*, vol 5, Rabek, J F (ed), CRC Press, Boca Raton, Florida, 1992, chapter 4, pp 103-185, and references therein
120. Flytzanis, C In: *Quantum Electronics, A Treatise*, vol 1, Rabin, H and Tang, C L (eds), Academic Press, New York, 1975
121. Ledoux, I, Josse, D, Fremaux, P, Piel, J-P, Post, G, Zyss, J, McLean, T, Hann, R A, Gordon, P F, and Allen, S *Thin Solid Films*, 1988, 160: 217
122. Decher, G, Tieke, B, Bosshard, C, and Gunter, P *Ferroelectrics*, 1989, 91: 193
123. Aktsipetrov, O A, Akhmediev, N N, Baranova, I M, Mishina, E D and Novak, V R *JEPT Lett.*, 1983, 37: 207
124. Bubek, C, Laschewsky, A, Lupo, D, Neher, D, Ottenbreit, P, Paulus, W, Prass, W, Ringsdorf, H and Wegner, G *Adv. Mater.*, 1991, 3: 54
125. Allen, S, McLean, T D, Gordon, P F, Bothwell, B D, Robin, P and Ledoux, I *SPIE Proc.*, 1988, 971: 206
126. Nalwa, H S, Watanabe, T, Nakajima, K and Miyata, S In: *Proceedings 5th Toyota Conference on Nonlinear Optics*, Miyata, S (ed), Elsevier, Amsterdam, 1992, p. 271
127. Haung, J, Lewis, A, and Rasing, T J. *Phys. Chem.*, 1988, 92: 1756
128. Okada, S and Nakanishi, H *Surface*, 1989, 27: 957 (in Japanese)
129. Nalwa, H S, *Appl. Organomet. Chem.*, 1991, 5: 349
130. Wright, M E, Toplikar, E G, Kubin, R F and Seltzer, M D *Macromolecules*, 1992, 25: 1838
131. Richardson, T, Roberts, G G, Polywka, M E C and Davies, S G *Thin Solid Films*, 1989, 179: 405
132. Davies, S G, Richardson, T, Roberts, G G and Polywka, M E C European Patent EP-88-306310 (11 July 1988)
133. Sakaguchi, H, Nagamura, T and Matsuo, T *Jpn. J. Appl. Phys.*, 1991, 30: L377
134. Carr, N, Goodwin, M J, McRoberts, A M, Gray, G W, Marsden, R and Scowston, R M *Makromol. Chem., Rapid Commun.*, 1987, 8: 487
135. Nalwa, H S, Kakuta, A and Miyata, S *Nonlinear Optics of Organic Molecular and Polymeric Materials* CRC Press, Boca Raton, Florida, 1993
136. Sauteret, C, Hermann, J P, Frey, R, Pradere, F, Ducuing, J, Baugman, R H and Chance, R R *Phys. Rev. Lett.*, 1976, 36: 956
137. Carter, G M, Chen, Y J and Tripathy, S K *Appl. Phys. Lett.*, 1983, 43: 891
138. Kajzar, F and Messier, J *Thin Solid Films*, 1985, 132: 11
139. Kajzar, F and Messier, J *Thin Solid Films*, 1983, 99: 109
140. Chollet, P A, Kajzar, F and Messier, J *Thin Solid Films*, 1985, 132: 1

-
141. Kajzar, F, Messier, J, Zyss, J and Ledoux, I *Opt. Commun.*, 1983, 45: 13
142. Kajzar, F, Messier, J and Rossillio, C J. *Appl. Phys.*, 1986, 60: 3040
143. Embs, F W, Wegner, G, Neher, D, Albouy, P, Miller, R D, Wilson, C G and Screpp, W *Macromolecules*, 1991, 24: 5068
144. Shutt, J D, Batzel, D A, Sudiwala, R V, Rickert, S E and Kenney, M E *Langmuir*, 1988, 4: 1240
145. Nalwa, H S (ed), *Ferroelectric Polymers*. Marcel Dekker, Inc., New York, 1993 in press